OPTIMIZATION OF THE RIG FOR AN AUTONOMOUS SAILING VESSEL

Bachelor's final thesis

Facultat de nàutica de barcelona
Universitat politècnica de catalunya

Authors:
Martina Reche and Esperança Ruiz

Supervisor:
Javier De Balle

Bachelor's degree in naval engineering GESTN

Barcelona, June 2018

Nautical Science and Engineering Department

Acknowledgement

The authors would like to acknowledge the hospitality of all the people involved in the Maribot Vane team in the Maritime Robotics Laboratory in the Royal Institute of Technology (KTH). Big thanks to give us the opportunity to be a part of this awesome research project and learn that much from all of you. Especially, to Ulysse Dhomé and Jakob Kuttenkeuler.

Moreover, we would also like to acknowledge the support and patience shown of all the people working in the Maritime Robotics Laboratory and Aeronautical and Vehicle Engineering Department. Especially, to Stefan Hallström, Magnus Burman, Hans Liwång, Per Wennhage, Monika Norrby and Anders Beckman.

Furthermore, we would like to stress the fact that even though the distance has been an awkwardness, our supervisor, Javier De Balle, has always guided us through this project. Thank you very much for all the support, help and comprehension received.

Finally, big thanks to our family and friends to motivate us day after day to keep going on all what we have done.

Abstract

Due to the actual accelerating need for ocean sensing, autonomous vessels are able to play a key role in assisting scientists and researchers with collecting oceanographic data and environmental monitoring. That is why Maribot Vane project, an autonomous sailing drone, came up at the Maritime Robotics Laboratory at The Royal Institute of Technology (KTH). This vessel will be used as a sensor carrying platform for autonomous data acquisition in open waters. This sort of vehicle has higher potentials to be cheaper and a helpful alternative to ordinary commercial research vessels.

This bachelor's final thesis is performed in collaboration with the research group of the Maribot Vane project of KTH. Its aim is to develop a new concept for the existent flap (small back rigid sail which makes the autonomous vessel sail with nearly no energy needed) in order to improve the performance and the characteristics of the whole rig for this autonomous sailing vessel. The main goals are to create a robust, lightweight, waterproof and self-looking flap.

The thesis presents the requirements and the design, study, manufacturing and testing processes of the new concept of the flap.

The new concept of the flap shows promising results such as better aerodynamic behavior, better distribution of the weight and a completely watertight area for the electronics.

Contents

Chapter 1

Introduction

There is a growing need for ocean-based sensing in remote areas not accessible to most researchers. With the opening of Arctic waters and the changing weather patterns all over the globe, reaching new destinations to carry out research observations has become vital. The realization of an energy independent autonomous surface vessel, to act as a mobile research tool, has been targeted by the Maritime Robotics Laboratory at KTH, and the Maribot VANE project is the result.

The opportunities for an autonomous robotic sailboat are extensive. Applications such as long-term position bound environmental monitoring, shallow water mapping, multi-agent missions for fish tracking (to mention a few) is where this type of vessel can complement conventional research vessels and equipment in data acquisition. For weather data collection, while it is within satellite capabilities to gather some surface weather data, being able to reach areas of shallow water where data is not possible to be gathered by satellite is crucial.

This type of vessel would also be able to carry a payload of deployable sensors that could include data gathering aerial drones, or underwater instrumentation that could be deployed and regathered after any amount of time necessary for the mission objectives of the payload.

The main purpose of this autonomous sailing drone project is to offer a sustainable alternative for these autonomous missions by using wind and an energy efficient self-steering mechanism. The wind is the energy that propels the vessel and the stored energy is only used to change course and possibly send and receive data. That is why a flap is needed in the rig structure.

Generally, a flap is a type of high-lift device used to increase the lift of an aircraft wing at a given airspeed. Nevertheless, in this project, the flap is the little rigid wing mounted off the trailing edge of the also rigid main wing which creates the moment needed to move the main wing with nearly no energy needed.

The aim of this Bachelor's Final Thesis is to contribute in this research project designing and creating a new optimized flap for the Maribot VANE since the actual one does not perform that well. Improving the aerodynamic behaviour, gaining rigidity in the flap structure, having a watertight area to place the electronics and reaching a better distribution of the weight are some of the objectives pursued in this thesis.

Moreover, the fact that all the thesis is based on own research and imagination boosts more knowledge and experience in this field.

In order to achieve all exposed before, this Bachelor's final thesis is divided into four big chapters. The first one exposes the Maribot VANE Project in KTH in general, the second one, all the design process and manufacture of the new flap; the third one, the testing process of the new flap; and the last one, the discussion, conclusion and future work of the entire project.

Chapter 2

Maribot VANE

2.1 Design Mission Statement

The design mission of this research project of the Maritime Robotics Laboratory in KTH named Maribot VANE is to design and create an autonomous sailing drone for oceanic research. This vessel is supposed to be sailing on its own during several months with as little energy as possible. The route which is going to follow depends on the research project it is going to be related to.

2.2 Background

The Maribot VANE, the autonomous sailing drone for oceanic research, is a platform to measure data at sea. Depending on the research project which use the vessel, these data could be salinity, temperature, meteorology and fish-tracking for instance. This project came up in the Maritime Robotics Laboratory in KTH as the response to the growing need for ocean based sensing in remote areas to most researchers and as an environmental-friendly alternative to the actual vessels that carry this function.

This platform is intended to be sailing autonomously for several months. Thus, it has to be robust to withstand any weather conditions.

One of the two main features of the Maribot VANE project is the rigid free-rotating rig system, which is used to propel the vessel. The rig is self-adjusting, free to rotate 360 degrees and it is able to adjust the angle of attack automatically using a single actuator where no sheets or halyards are needed, which differs substantially from a conventional sailboat.

The second main feature is that the rotation of the wing is coupled to the boat rudder to keep a constant apparent wind angle. The rig is equipped with a control surface, here denoted flap, the object of study of this bachelor's thesis. In other words, this autonomous sailing drone is self-adjusting, it has no active control of the wing angle but the wind trims it, and self-steering, most of the time it is not actively steered to consume less energy.

The general specifications of the Maribot VANE are presented in Table 2.1 below.

General specifications	
Length over all	4.2 m
Width	0.8 m
Height above waterline	4.0 m
Displacement	280 kg
Material	GRP
Free-rotating rig	
Span	3.5 m
Area	3.0 m2
Weigth	25 kg
Material	GRP, PVC core
Flap Control	Linear actuator

Table 2.1: General specifications

The VANE is composed of six main parts, which are showed in the Figure 2.1:

- Rigid free-rotating rig **(1)**: the rig is free to rotate 360º. Acts as a wind vane.
- Flap **(2)**: controls the angle of attack of the main wing and gives stability to the whole rig.
- Mass balance **(3)**: keeps the rig mass stable to prevent boat motion to affect the angle of attack.
- Wind-rudder **(4)**: energy efficient solution of self-steering.
- Electronics **(5)**: in-house developed electronics to control the boat.
- Wind measurement and telecommunication **(6)**: anemometer and antenna.

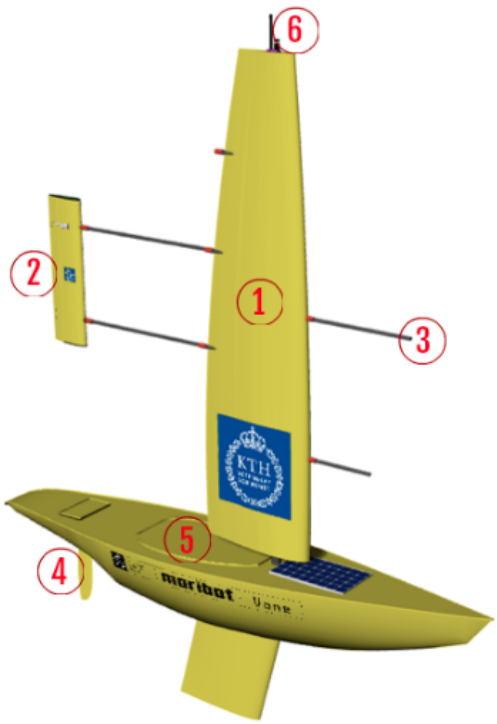

Figure 2.1: Parts of the Maribot VANE. Source: Tretow, C, 2017, Design of a free-rotating wing sail for an autonomous sailboat, Master's thesis report, Centre for Naval Architecture, KTH Royal Institute of Technology, Stockholm.

2.3 Rig operating principle

This section presents the operating principle of the Maribot VANE's rig. This knowledge is really important in order to be able to understand this entire Bachelor's Final Thesis.

As said before, Maribot VANE is fitted with a rigid symmetric free-rotating rig composed of two parts: the main wing and the flap. The entire rig rotates around a common axis, i.e the mast, placed at the chord-wise center of pressure of the main wing. The operating principle of the rig relies on the flap. The flap is the part of the rig which, by adjusting its angle, sets the rig to a certain angle of attack.

In order to explain step by step the rig operating principle, an ideal state is taken: the angle of attack is 0 and both profiles are not creating any lifting force due to their symmetric profiles. When the main wing is supposed to be moved, the flap has to be deflected first. The actuator deflects the flap. Due to this deflection (different angle of attack) and the profile of the flap, the flap creates a lifting force. This lifting force creates a rotational moment around the common axis of rotation which forces the main wing to rotate too. The area of the flap is designed so that the equilibrium of rotational moments (the one created by the flap and the one created by the main wing) reaches the zero value when the desired angle of attack in the main wings is set. This equilibrium of moments is maintained regardless of wind speed and direction. Figures 2.2 and 2.3 show this principle.

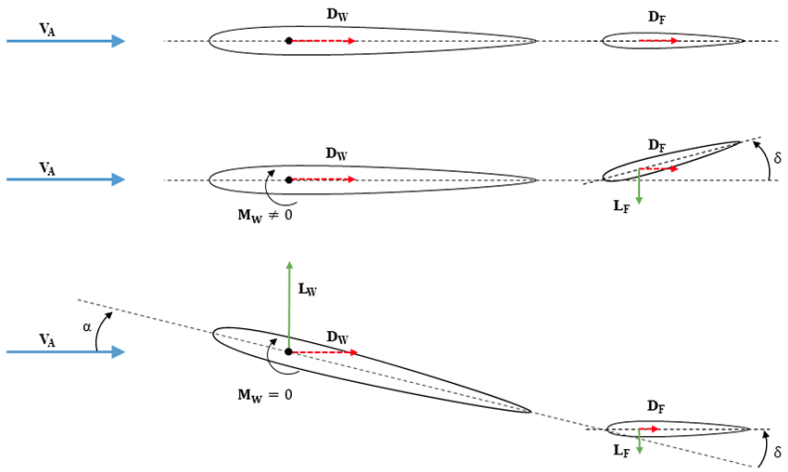

Figure 2.2: Sketch of the rig operating principle step by step

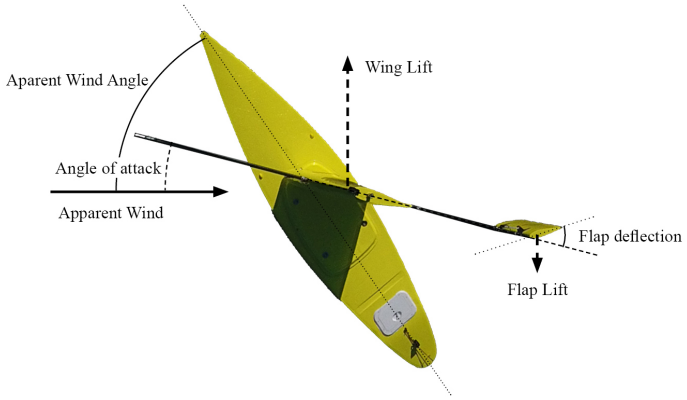

Figure 2.3: Sight from above with the forces actuating in the wing marked. Source: Tretow, C, 2017, Design of a free-rotating wing sail for an autonomous sailboat, Master's thesis report, Centre for Naval Architecture, KTH Royal Institute of Technology, Stockholm.

Moreover, the flap has a second role. This role is acting as the rig tailplane, generating rig rotational restoring torque whenever the apparent wind direction changes. The flap is able to make the whole rig follow the wind.

The flap actuator is connected to the main micro-controller which is the responsible of giving the information when the flap has to be deflected or maintained in its position.

2.4 Actual flap

In order to be able to do its two main functions, the actual flap:

- Controls the angle of attack of the main wing.
- Is attached and connected with the actuator.
- Is attached to the main wing.
- Is lightweight (low impact on the overall mass balance/stability).
- Has a variable flap lever arm (adjustment capabilities for experimental testing of optimal flap position)

As it is shown in the previous figures (2.1,2.2 and 2.3), the flap has a rectangular shape with a NACA 0018 profile (symmetric profile). It is attached parallel to the sea line to the main wing with two carbon fiber rods. These rods are able to be placed furtherer or closer to the main wing giving the flap a variable lever arm.

After testing the vessel, it was observed that the flap could be placed as close as possible to the main wing and the rig was still performing well. The minimum distance achieved was 108cm from the axis of rotation (mast) to the leading edge of the flap. This distance limit is because of the linear actuator which is placed on the rods.

Latex Vortix Method has been the method used to calculate the actual dimensions of the rig and its position, which are the following ones:

Flap specifications	
Flap aerodynamic profile	NACA 0018
Flap area	0.368 m2
Flap aspect ratio	1
Flap taper ratio	5
Flap span	1.175 m
Flap chord	0.31 m
Flap weight	1.5 kg

Table 2.2: Flap specifications

In terms of materials, the core of the flap is made of Divinicell H35 and H100 joined together with adhesive Epoxy resin, Huntsman RenLam LY113. The core is reinforced with one layer of thin Sartex fiberglass, one layer 421 g/m2, [0 90] layer up. The fiberglass is laminated with a layer of resin mixed with aerosil. The rods are carbon fiber tubes with 29.5 mm of diameter.

Attached to the upper rod there is a linear actuator that makes effective the movement of the flap. The actuator is able to hold its position when power is removed and has potentiometer position feedback. The linear actuator used is a L16-P with a 10 mm stroke length. Is mounted with 3D printed parts to the flap. The control and power cables are routed through the internal structure to a watertight compartment placed in the hull, containing a control board, batteries and RC-receiver.

Chapter 3

New flap

3.1 Requirements

In order to design something new for this project, the requirements to fulfill are a must. The ones of the new flap are the followings:

- The flap should be capable of effectively generating a moment so that the rig is rotated to a desired angle of attack (around 12 degrees).
- The flap should be capable of holding its position without any-power consumption.
- When the wing is exposed to a disturbance, such as a change in wind angle, the flap should be able to give a large restoring moment to stabilize the wing so that it reaches equilibrium again.
- The flap should be a lightweight and robust structure.
- The flap should be capable of keeping all the electronics needed to be moved protected from the water.
- The flap should be capable of being connected/attached to the main wing.
- The flap should have a shock absorption system.
- The flap should be removable.

3.2 Brainstorming

Focusing on fulfilling all the requirements exposed previously, these three ideas came up while the brainstorming was taking place.

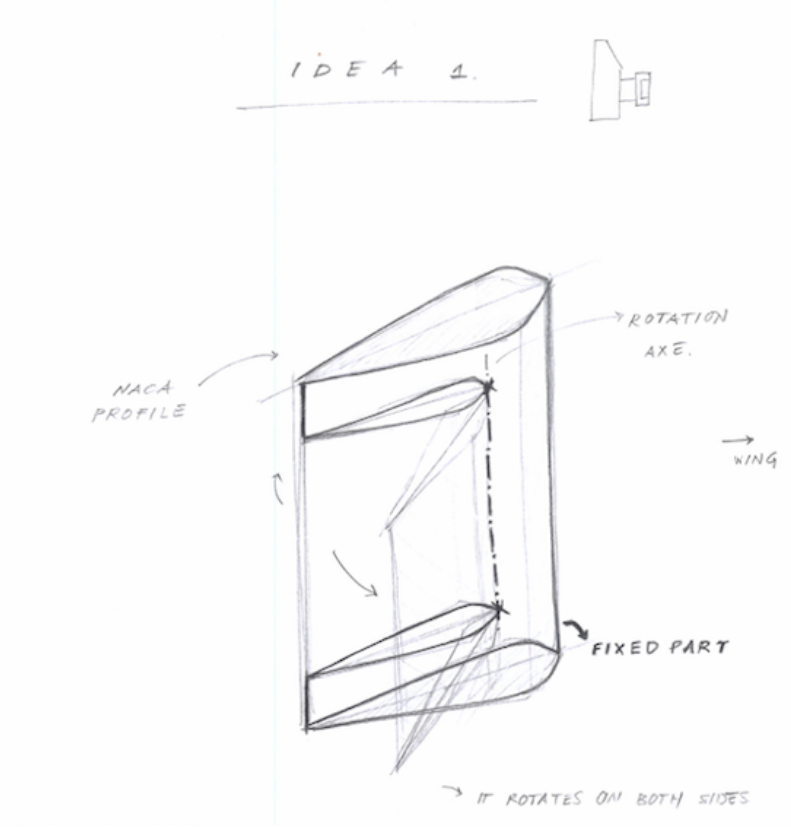

Figure 3.1: First idea

This first proposal is based on keeping the same idea of the old flap but creating another flap above it in order to create a waterproof structure where the actuator and all the electronic devices needed to create movement, could be placed inside.

From an aerodynamic point of view, this shape would acts as a non symmetric profile creating a much higher value of Cl. Thus, more lift for less area. However, the non-mobile part of the flap, the outside case, would create a lift in the same direction of the main wing and contrary to the one created by the flap.

As seen in the drawing, the axis showed has two main functions: to connect both structures (outside case and flap) and to be the rotation axis of the flap.

Keeping in mind all the requirements to fulfill, the following table shows the pros and cons of this first flap idea compared to the old and existing one.

Pros	Cons
Robustness	Difficult to built
Waterproof	Not lightweight
More lift for less area	Some lift created in the same direction of the main wing
Design more revolutionary	More material needed
Able to reach the actuator from outside	More expensive
	Few space to place the actuator

Table 3.1: Pros-Cons of the first idea

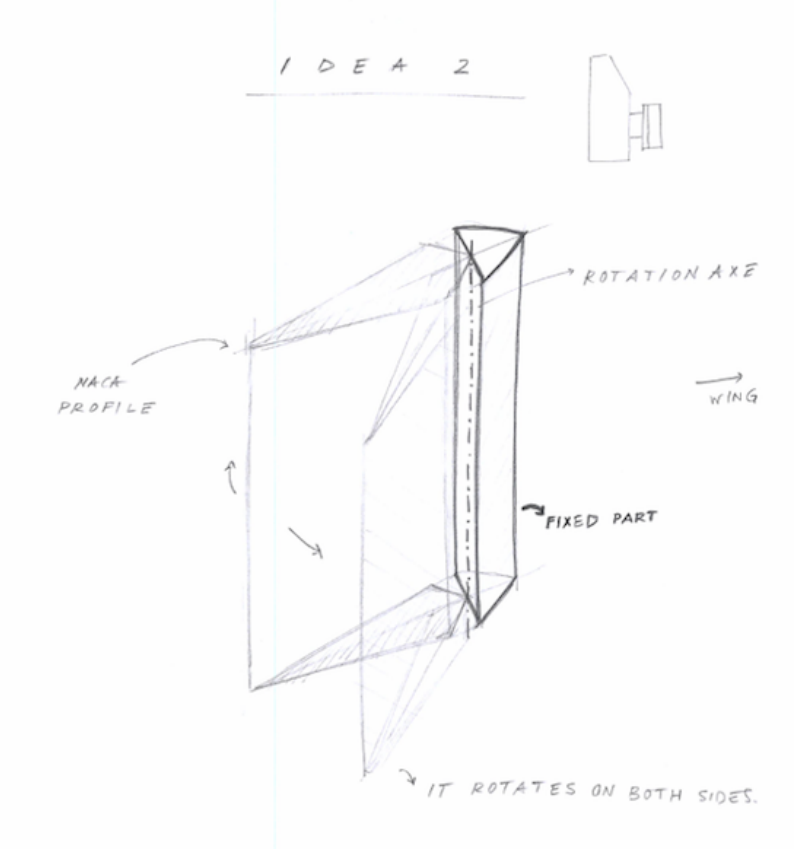

Figure 3.2: Second idea

This second proposal is based on also keeping the same idea of the old flap but creating a front fixed part in it. In this front case, the actuator and all the fragile devices needed to generate the movement.

From an aerodynamic point of view, this shape would acts as a non symmetric profile creating a much higher value of Cl. Thus, more lift for less area. Moreover, in contrast to the first idea, in this design there is no part creating lift in the other direction.

Nevertheless, in this concept, the lever arm that transmit the movement from the actuator to the axis of rotation would not be protected inside the front case.

Keeping in mind all the requirements to fulfill, the following table shows the pros and cons of this second flap concept compared to the old and existing one.

Pros	Cons
Robustness	Difficult to built
More lift for less area	Not lightweight
	Partly waterproof
	More material needed
	More expensive

Table 3.2: Pros-Cons of the second idea

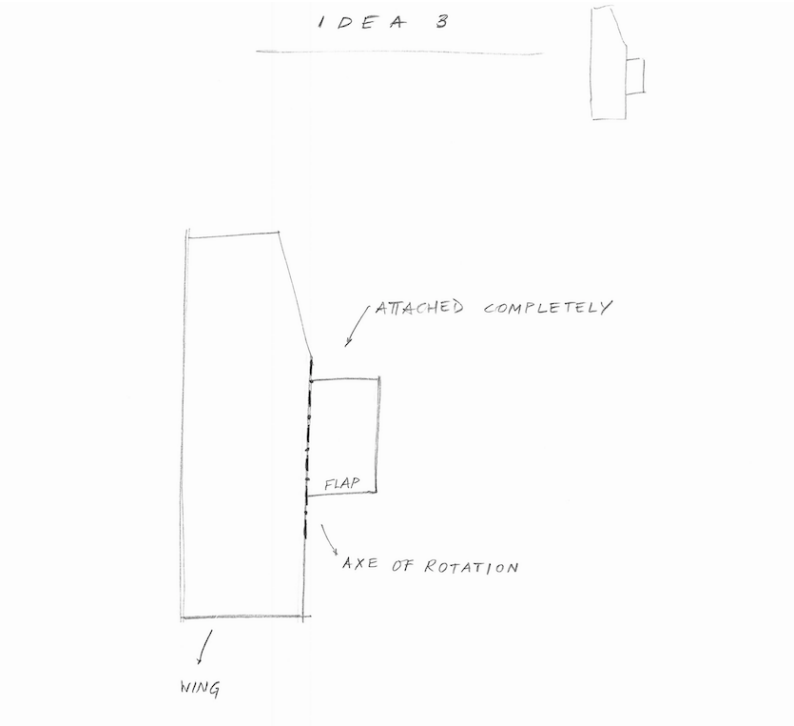

Figure 3.3: Third idea

In this third proposal, the idea of attaching the flap to the main wing has appeared. With this idea, the main wing and the flap would be all in one piece giving more robustness to the entire structure. The actuator and all the fragile devices could be placed inside the main wing.

However, the behavior of this flap is a bit complicated and there is no clear evidence that it would work perfectly. The flap is not sure to be able to performance its two main functions: following the wind (giving stability) and created the moment needed to move the rig.

To sump up all the pros and cons of this proposal, here it is the following table.

Pros	Cons
Robustness	Not sure it could work (flap performance)
Waterproof	
Lightweight	

Table 3.3: Pros-Cons of the third idea

3.3 Final idea

After all ideas proposed it has been known that the best solution is to have the axis of rotation of the flap in the edge of the main wing.

With this proposal, rod plus flap is going to be just one piece. Thus, the actuator and electronics can be placed inside the main wing. This concept fulfills at first sight at least three of the main requirements of the project: lightweight, robustness and waterproof.

The best option for the new flap design is shown in the following figure 3.4:

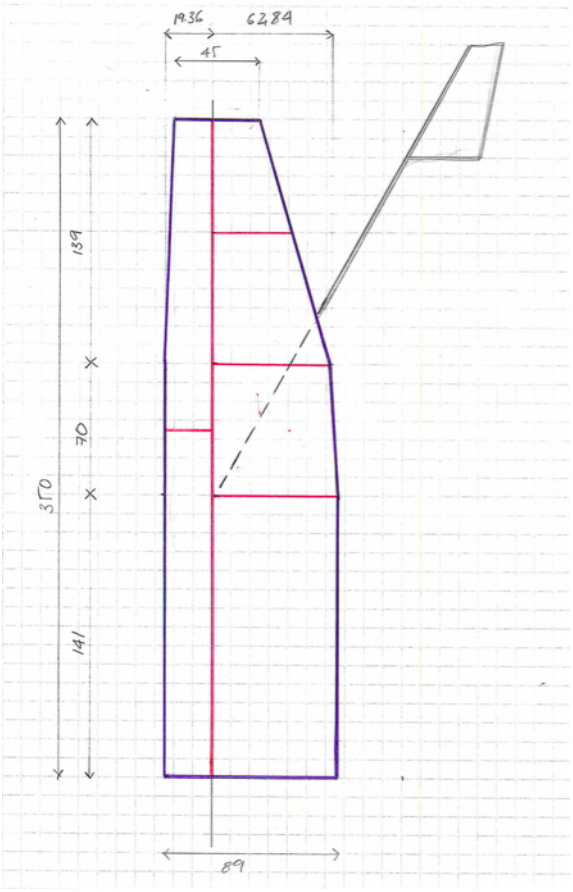

Figure 3.4: First sketch of the final idea

The flap is attached with only one rod which is the axes of rotation of the flap. All the mechanisms and electronics are placed inside the main wing with a waterproof system in the edge of the wing and, thus, protected from the environment.

In the main wing there will be a hatch in order to be able to reach the motor. Through the hatch, the flap is going to be released in case it's needed to transport the Maribot VANE.

3.4 Aerodynamic study

In order to be able to optimize the existent flap and create a new concept based on the design presented above (3.3 Final Idea), an aerodynamic study is needed. In this part, what is pursued is finding out how the flap has to look like in order to be as aerodynamic as possible (create maximum lift per minimum surface).

Furthermore, this study is based on reducing the weight of the flap, fulfilling the lightweight requirement.

The first part needed is the profile of the flap. In order to fulfill the lightweight requirement, a reduction of the NACA profile could be a good idea since the thickness would be reduced and, at the same time, for small angles of attack ($\leq 5^{o}$), a slim profile, NACA 0012 for instance, is more aerodynamic (creates more CL for the same angle of attack) than the thick ones, NACA 0018 in this case.

In the following two graphs, this is shown.

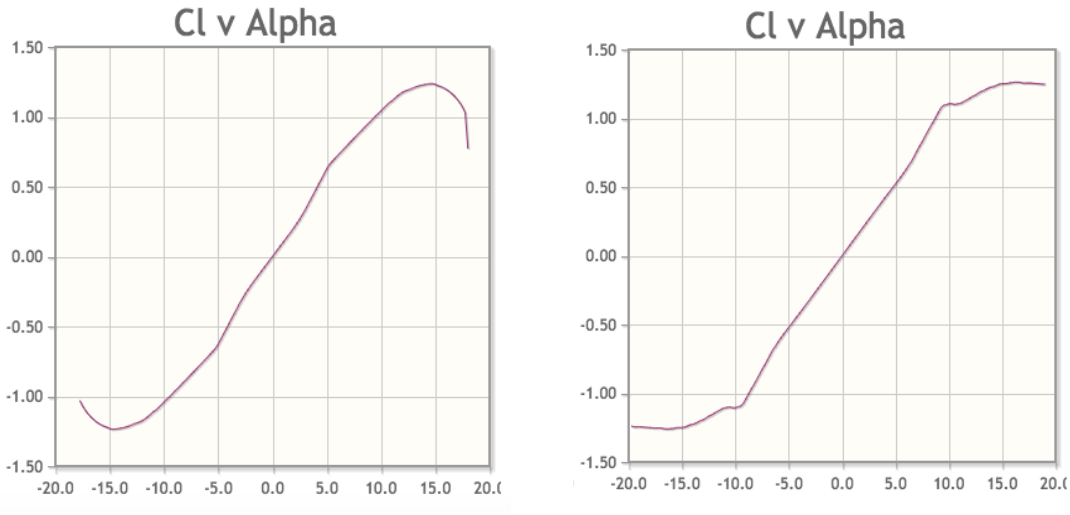

Figure 3.5: Comparative between the Cl curve depending on the angle of attack for the same condition, 500.000 Reynolds. On the left side, the graph of a NACA0012 profile is shown and on the right, the NACA0018 one. As it is seen, the Cl value is higher in the slimmer profile while the angle of attack is $\leq 5^{o}$. Source: www.airfoiltools.com

However, due to the angle of attack, angle between the chord of the profile and the apparent wind (AP), needed (angle of attack of the actual flap is 3^{o}) is quite close to the limit and in some cases it can be bigger than the limit, this option has been discarded. If the thickness is reduced, an area increase is needed.

So, there is no advantage on that. For all these reasons, the NACA 0018 profile is going to be maintained as the profile of the new flap.

The other aspect needed to be calculated is the minimum area needed in order to have equilibrium between the flap and the main wing. This equilibrium is needed when the angle of attack of the main wing is 12 degrees. With this angle of attack for the main wing, a good lift coefficient is reached while staying in a safe position where the main wing does not stall. Thus, a good lift is created.

In order to solve this problem, finding out which is the minimum mass required to reach this position, an equilibrium of moments calculation is needed. 16 degrees of deflection of the flap is taken (degrees between the chord of the main wing and the chord of the flap), creating 4 degrees of angle of attack on it.

Before starting with the calculation, a draft of the position of both wings is showed (Figure 3.6):

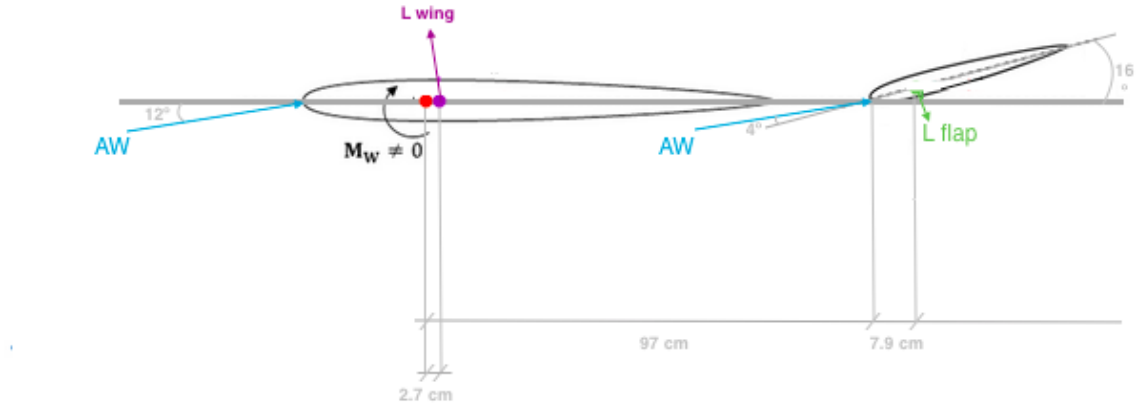

Figure 3.6: Draft of the equilibrium situation. The angle of attack, angle between the apparent wind (AW) and the chord of the profile, of both wings and the deflection of the flap are shown. Furthermore, the distances where the lift forces are created.

It is general knowledge that equilibrium is a state in which opposing forces or influences are balanced. In oder words, the sum of moments must be 0.

In this system, there are two wings so, two lifts created with two different distances from the axis of rotation of the whole rig.

$$\Sigma M = 0 \tag{3.1}$$

$$(L \cdot d)_{mainwing} = (L \cdot d)_{flap} \tag{3.2}$$

$$(\frac{1}{2} \cdot \rho \cdot v^2 \cdot s \cdot Cl \cdot d)_{mainwing} = (\frac{1}{2} \cdot \rho \cdot v^2 \cdot s \cdot Cl \cdot d)_{flap} \tag{3.3}$$

Considering the same air density and speed,

$$(s \cdot Cl \cdot d)_{mainwing} = (s \cdot Cl \cdot d)_{flap} \tag{3.4}$$

Taking into account the angles,

$$2.7m^2 \cdot 1.1 \cdot \cos 12^o \cdot 0.027m = s \cdot 0.4 \cdot \cos 4^o \cdot \cos 16^o \cdot (0.97m + 0.08m \cdot \cos 16^o) \tag{3.5}$$

$$s_{flap} = 0.196m^2 \tag{3.6}$$

As seen in the following graph (Figure 3.7), the Cl of each angle of attack is the one showed in the equations above.

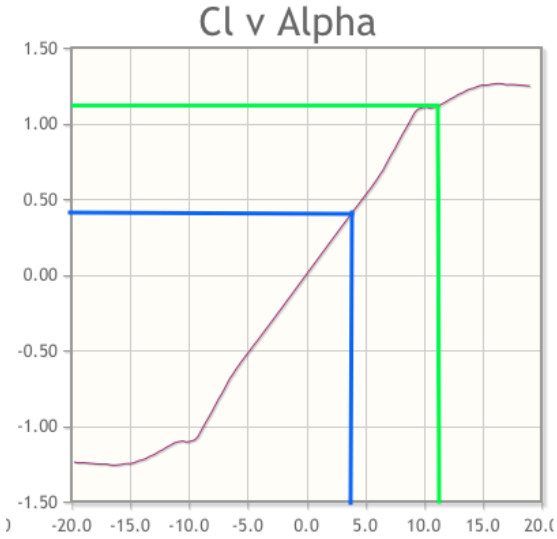

Figure 3.7: Graph Cl-Angle of attack for a NACA 0018. In green, for an angle of attack of 12º (main wing) and in blue, for a angle of attack of 4º. Source: www.airfoiltools.com

In order to overestimate the flap area, a final value of 0.23 m^2 has been taken. With this aerodynamic study the flap area has been reduced from 0.37 m^2 to 0.23 m^2 (around a 38 % less) and the optimization of the actual flap has started.

3.5 Load Study

In order to know the loads the flap will be able to resist, a load study is needed.

When sailing, due to the movement, the fluid flowing past the surface of the body (the flap) exerts a force on it. Lift is the component of this force that is perpendicular to the oncoming flow direction (apparent wind). This force depends on the density of the air flow, the speed of it, the surface of the body, the kind of the profile and the angle of attack. It creates the force that pushes the profile up.

It contrasts with the drag force, which is the component of the force parallel to the flow direction. The drag is the force that the profile generates to make resistance against its own creation of the lift. In order words, to make resistance against its movement. This opposite force also depends on the density of the air flow, the speed of it, the surface of the body, the sort of the profile and the angle of attack. The ideal profile would be the one that will not create any kind of drag force when lift will be generated.
Furthermore, in static condition, even if there are no lift and drag created, the weight of the structure acts.

In each profile, the resultant force, the sum of all these forces, is applied in the same point, the center of pressures. The center of pressure on a symmetric airfoil typically lies close to 25% of the chord length behind the leading edge of the airfoil. This is called the "quarter-chord point".

For a symmetric airfoil, as angle of attack and lift coefficient change, the center of pressure does not move. It remains around the quarter-chord point for angles of attack below the stalling angle of attack.

Taking into account all said before, the main loads applied in the flap are: the lift and the drag (aerodynamic forces) and the weight (mass force).

In the following figure, the distribution of the main forces and its application point (Center of pressures) are shown.

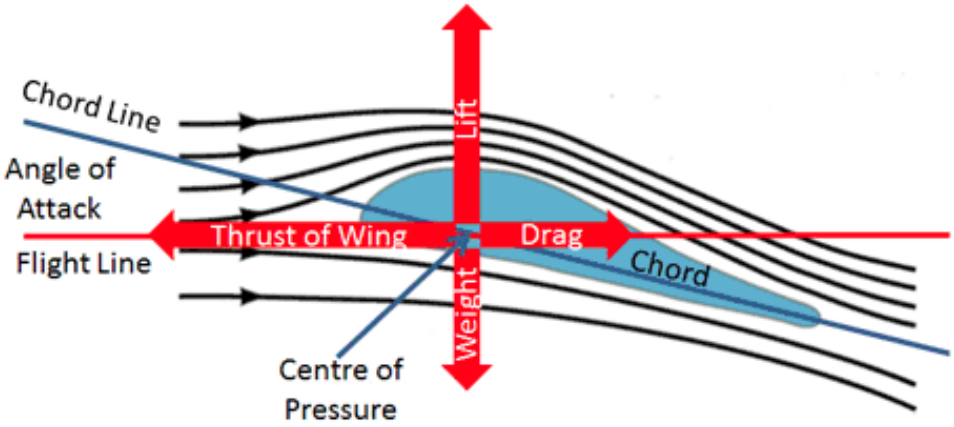

Figure 3.8: Non-symmetric airfoil profile sketch where the main characteristics of it are shown. Source: www.grc.nasa.gov

In order to know the values of the forces applied in the flap surface and, in consequence, knowing which forces it has to resist, the aerodynamic forces, lift and drag, are first calculated. Since, this forces are needed to design the flap, the calculations done are for the worst weather situation. This condition is when the Maribot VANE will face a real wind of 60Kn. In the scale of Beaufort, wind scale, 60Kn is considered as a hurricane storm. So, the maximum wind that the sailing drone could face.

It is known that the lift created in a NACA profile is equal to:

$$L = \frac{1}{2} \cdot \rho \cdot v^2 \cdot s \cdot Cl \tag{3.7}$$

where in the worst condition considered:

ρ = density of the air = 1.225 Kg/m^3
v^2 = wind speed = 60 Kn = 30.86 m/s
s = flap area = 0.23 m^2
Cl = lift coefficient = 0.4 (for 4 degrees of angle of attack, taken from the graph of above (figure 3.7))

The value of lift created for this condition is:

$$\textbf{L=54.18N} \tag{3.8}$$

The resultant lift force is created in the 25% of the chord and perpendicular to the direction of the apparent wind in each NACA profile. Thus, the resultant lift of the entire flap, the sum of the lift of each profile, can be also considered created in the 25% chord line at the height of the center of gravity. In this new flap concept, this point is around 1 meter far from the axis of rotation (mast) and is named the center of pressure of the entire flap.

In consequence of this lift created by the profile of the flap, the drag generated is equal to:

$$D = \frac{1}{2} \cdot \rho \cdot v^2 \cdot s \cdot Cd \tag{3.9}$$

where in the worst condition considered:

ρ = density of the air = 1.225 Kg/m^3
v^2 = wind speed = 60 Kn = 30.86 m/s
s = flap area = 0.23 m^2
Cd = drag coefficient = 0.009 (for 4 degrees of angle of attack, taken from the following graph (figure 3.9))

The value of drag created for this condition is:

$$\textbf{D=1.21N} \tag{3.10}$$

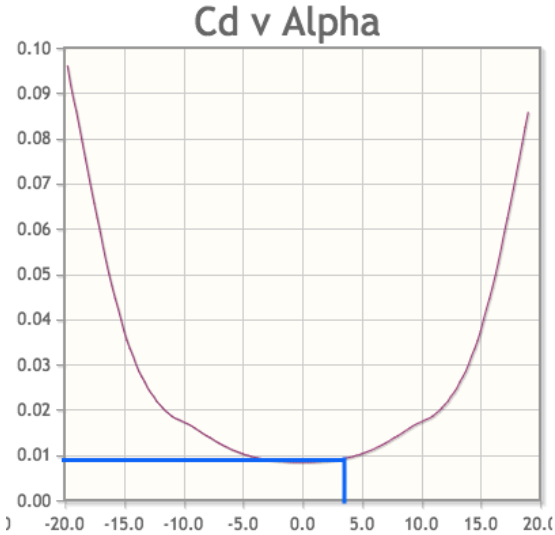

Figure 3.9: Graph Cd-Angle of attack for a NACA 0018. In blue, for a angle of attack of 4º. Source: www.airfoiltools.com

The resultant drag force is created in the same place as the resultant lift force but in a different direction. Instead of perpendicular to the airflow, as said before, its direction is parallel to it.

As seen, since it is a NACA profile airfoil, the value of drag generated is much lower than the lift. In other words, it is aerodynamic.

The last force applied which has been mentioned is the weight. The final weight of the flap is hard to know because since it is hand made, until the end it is not exactly known. However, it is considered around 1 Kg (10 N). Even though the value could be approximately known, as the rest of forces calculated, its direction makes it negligible. The total lift and drag actuate perpendicular to the lateral surfaces but the weight, as its naturalness indicate, on the lower one. So, it will be compensate by the same rod holding structure inside the main wing not the flap structure itself as the other aerodynamic forces. Just in the rod selection, it has to be taken into account but it is a really small force.

Finally, just taking into account that the flap will experience several efforts like torque and compression and these will create responses such as deflection. This deflection, in order to have a robust and long-lived structure, has to be as small as possible.

Maintaining the original shape also provides the same optimal performance of the designed one.

3.6 Design process

The explanation of the design process of the new flap is exposed in this section.

3.6.1 Area

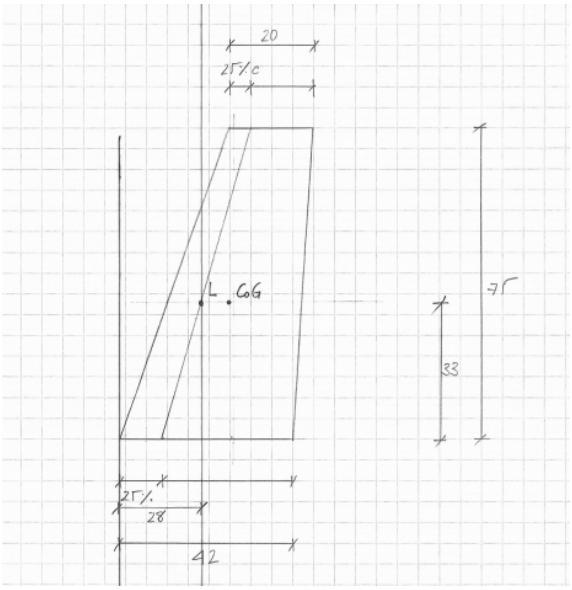

Figure 3.10: Hand draft with the main dimensions of the flap.

The previous image shows the chosen dimensions for the flap. The area required for the proper movement of the rig is calculated in the previous point (3.4 Aerodynamic study) is 0.18 m2. The final area of the flap is 0.23 m2 with a margin of 22 per cent.

This oversizing is needed because of:

- The aerodynamic calculations are made by hand. They cannot be super precise since potential flow which is a model and not exactly real life is used.
- It is considered a laminar flow for the aerodynamic study. The shielding of the main wing and, thus, the disturbance of the inflow of the flap is not taken into account.
- The flap is hand made. The NACA profile of the flap is not perfect, it has some small imperfections which make that the lift created might differ from the theoretical value.

Geometric specifications	
Profile	NACA0018
Span	75.0 cm
Root chord	42.0 cm
Root maximum thickness	7.6 cm
Tip chord	20.0 cm
Tip maximum thickness	3.6 cm
Leading edge angle	70º
Trailing edge angle	3.8º
Aspect Ratio	2.4
Taper Ratio	0.5

Table 3.4: Geometric specifications

The aspect ratio and the taper ratio contribute in the aerodynamic and structural properties of the wing.

The aspect ratio AR is ratio of the square of the wingspan b to the projected wing area S.

$$AR = \frac{b^2}{S} \tag{3.11}$$

The new flap has an aspect ratio of 2.4, half of the aspect ratio of the previous flap. A long wing has higher bending stress for a given load than a short one and therefore requires higher structural-design specifications. With a shorter span the bending stress and also the torsion can be avoided.

The taper ratio TR is defined as the relation between the chord at the tip Ct and the chord at the root Cr.

$$TR = \frac{Ct}{Cr} \tag{3.12}$$

The previous design did not have taper ratio, on the contrary, the new flap has a pronounced aspect ratio; 0.5. Tapered wings increase the aspect ratio of the wing (length to chord width) improving lift.

3.6.2 Rods

As mentioned before, the lift line is at the 25 per cent of the chord from the leading edge. The lift point is determined by the intersection between the lift line and the longitudinal center of gravity of the flap.

The main point of this sailing drone is to consume little energy. The position of the rod in relation to the flap is conditioned by this principle. The rod crosses the aerodynamic center. Therefore, theoretically the torque needed to rotate the flap is zero. The torque needed is directly proportional to the distance of application of the force. In practice, the torque needed to rotate the flap will not be zero since the flap is going to be done by hand.

The rod has the same inclination of the leading edge of the flap: 70 degrees.

Two types of rods will be used. One wider in order to place it inside the other.

The flap is assembled to one rod which is fixed inside the main wing. The outer diameter of the rod of the flap is 29.5mm, little smaller than the inner diameter of fixed rod (the one inside the main wing) which is 29.9mm. The rod of the flap rotates inside the fixed rod, which acts as a rail. Both are carbon fiber rods from Carbix (Swedish company, carbix.se). The friction coefficient between them is nearly zero, the power used to rotate the flap is not going to be affected by this connection system.

See 7.6 Appendix F. Study of the bending stress and deflection of the rods, for more information about it.

3.6.3 Materials

After evaluating different materials, carbon fiber is the best option due to its properties in relation to our requirements. High Strength to weight ratio and rigidity are the main advantages that carbon fiber offers.

When designing with carbon fiber, one of the most important considerations is knowing the direction of the property of interest. Unlike metals, carbon fiber, and composites in general, are anisotropic. This means the properties of the material are directionally dependent.

Several tests have been done to decide which behavior is the most suitable for the prototype.

The Vacuum Infusion Process is one of many closed mold processes. It distinguishes itself by being the only process that utilizes only atmospheric pressure to push the resin into the mold cavity where the fibers are placed. The possibility of using prepreg carbon fiber was looked at.

Pre-preg is "pre-impregnated" composite fibers where a thermoset polymer matrix material, such as epoxy, is already present. The fibers often take the form of a weave and the matrix is used to bond them together and to other components during manufacture. The thermoset matrix is only partially cured to allow easy handling. Is a high-performance reinforced material that is used in racecar bodies and aircraft fuselages-plus prosthetic and orthotic devices. Composite structures built of prepregs will mostly require an oven to cure. This option had to be discarded due to the size of the oven of the laboratory.

The most common carbon fiber weave are the following ones:

1. Unidirectional (all fibers are parallel). In a 0-degree orientation, aligned with the fibers, unidirectional (UD) carbon fiber provides high bending strength against the progression of forces. In a 90-degree orientation, perpendicular to the fibers, it flexes. In either orientation, it has low torsional strength. In all

applications, another layer of fibres must be laid under, over or both sides of UD carbon-fiber weave.

2. Bidirectional (fibers cross at a 90-degree angle). In a 0-degree or a 90-degree orientation, bidirectional carbon fiber features medium bending strength and medium torsional strength. At a 45-degree orientation, it is more flexible and has high torsional strength.

It is possible to tailor the composite's properties with fiber length, the type of weave, fiber orientation, the number of layers, and the resin system to modify the component's capability to bear mechanical loads. Three tests with different combinations have been done:

- The first one is more focused on the lightweight requirement. It is used a really lightweight woven 0/90 fabric with 76 g/m2 of mass per layer. The orientation of the weaves is the 0 fibers following the leading edge of the flap. Two layers with the same orientation is the final decision for this first test. Unfortunately, two are the problems found with this lay up. The woven weave is really difficult to impregnate with the vacuum infusion system so, it doesn't cure properly. Otherwise, the fabric is too much light and the thickness is too thin to handle the loads already estimated for the flap.

Figure 3.11: First prototype

- For the second test, another kind of fibers have been chosen. A heavier 0/90 fabric with the fibers stuck to each other instead of woven (like in the previous test). The weight of the fabric is 400 g/m2. The orientation of the weaves is the 0 fibers following the leading edge of the flap. The two weaves have been placed upside down. This is: 0/90/90/0 to have symmetry with respect to the neutral axis of the lay up. In the case that the lay up is not symmetrical there is high probability that the shells twist after being removed from the mold.
  Besides, three foam ribs (Divinicell H100 with 1 cm of thickness) are placed above the two layers of carbon fiber and on top of each rib, an small piece of UD; working as stiffeners with a sandwich structure.

For this second test: the rod crossing the flap is avoiding the bending stress, the 0/90 fabric acts against the shear strength and the torsion and the stiffeners avoid the transversal stress. The result is something close to the expected shells for the flap. But after some tests, it is realized that some more stiffeners are needed because it is still too weak.

Figure 3.12: Second prototype

- For the third test test the tendency is to continue with the stiffeners, add a few more but here comes into play the possibility of using a more reinforced fabric and the weight that would have added with the other stiffeners are equivalent to the added by the fabric. With this prototype only carbon fiber acts, the idea sought from the beginning. The chosen fabric is 0/45/90/-45 with 440 g/m2 of mass.

  As in the following test, the final lay up is two layers places upside down in order to have symmetry with respect of the neutral axis of the lay up. This is: 0/+45/90/-45/-45/90/+45/0.

  The result of this third test is the expected one: the rod crossing the flap is avoiding the bending stress, the 0/90 fibers act against the shear strength and the torsion and the +45/-45 fibers avoid the transversal stress. With the result of the shells is the expected and we assemble the flap with them.

Figure 3.13: Third prototype

To assemble the shells and also the rod, two foam pieces are placed in the lower and the upper part. The foam used is Divinicell H100.

Next step, after everything is assembled, is testing it in real conditions in the Baltic Sea (See Chapter 4: Testing process).

3.6.4 Hatch

The hatch is built whit a squared retail of the main wing (made with carbon fiber). The retail is mounted on a smaller piece of foam. There are four screws on the sides where there is just carbon fiber. Two on each side. The hatch needs to be watertight so an o-ring is placed in the inner part of the screws (in the part where there is no foam). This is done to avoid the water going through the joints between the screw and the same hatch.

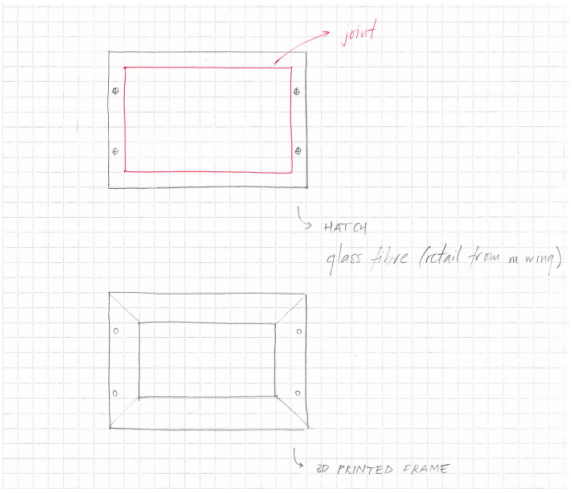

Figure 3.14: Sketch of the hatch

3.6.5 Waterproofing System

In order to protect the whole interior of the main wing from water, a waterproofing system, where the carbon fiber rod come out from it, is needed. The design of it is shown in the following figures 3.15 and 3.16.

This waterproofing system is going to be attached to the thinner rod. Its shape, as seen above, is going to let the thinner rod to get attached to the wider and, at the same time, permitting the movement between both of them. It is going to be made by PLA (Polylactic acid) using a 3D printer. In the interior, there are two notches where o-rings will be placed to better attach this system to the rods.

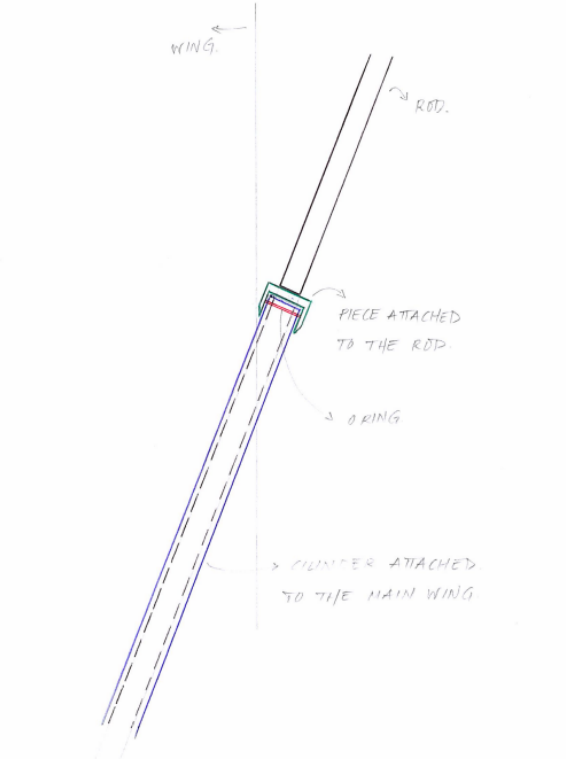

Figure 3.15: Sketch of the rod waterproofing system

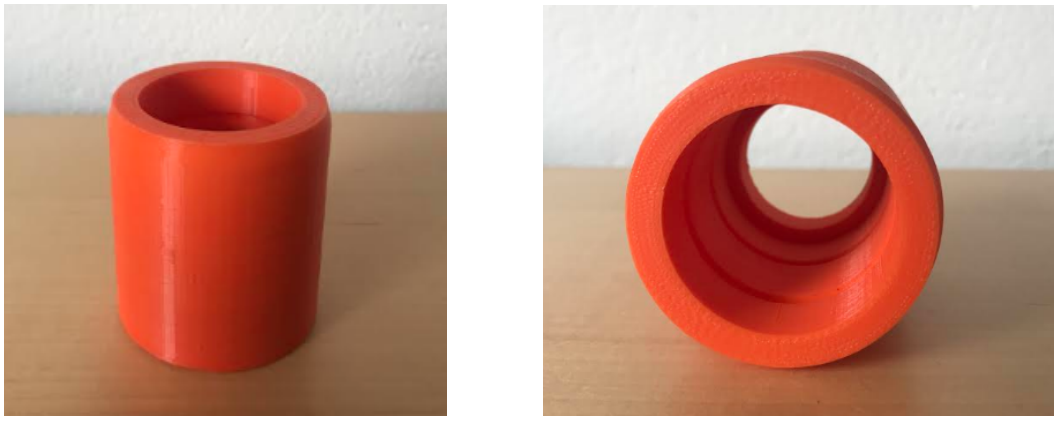

Figure 3.16: Pictures of the real waterproof system

3.6.6 Electronics

Inside the hatch, protected from the outside, is where the electronics, the most fragile part of this design, are placed. Their position is designed based on the transmission of the movement they create. From left to right, looking through the hatch of the main wing, the stepper motor with the worm as the output is first found. Then, the gear with a shaft as the output and the servo saver (shock absorption system). This last element, the servo saver, is attached to the gear using a shaft coupling. In the upper part of the servo saver, the rod of the flap is placed.

Its position is following an angle of inclination of -20º in order to the gear be perpendicular to the rod. The material that holds all the structure is foam.

Figure 3.17: Picture through the hatch of the real position of the electronics inside the main wing. As it is seen, instead of the stepper worm gear there is a linear actuator. That is because the gear did not arrive before the testing. However, in the near future, the actuator decided in this thesis, stepper worm gear, will be used.

See 3.7 Electronics for all the details about the electronics used and the design of the shock absorption system.

3.6.7 Attaching/Releasing the flap - operating principle

The servo saver design is the basis of the attaching/releasing the flap to/from the main wing operating principle. It, apart from its own function of protecting from damage the fragile parts, also permits the attachment between the rod of the flap and the actuator part. When needed to attach or release the flap to this part, with only using the hatch to reach this point and a simple clap it is going to be enough. Easy and fast.

In this operating principle of attaching or releasing the flap to or from the main wing, there is no need of assembling the electronics or any other component of the design every time a movement of the flap is needed. Only opening the hatch and opening or closing the clap placed in the upper part of the servo saver in order to release or attach the rod is needed.

3.7 Electronics

In order to be able to have movement in the new flap, some electronics are needed. As the requirement says, the flap needs to be moved a specific value of degrees in order to generate the momentum that creates equilibrium when the main wing has

an angle of attack of 12 degrees (ideal situation). Thus, the requirements of the electronics are:

- The electronics should be able to control and move the flap
- The electronics should be able to self-lock the flap
- The electronics should be able to have memory in order to know where the flap is all the time in case an impact moves it

The are some options which could be suitable for this flap. These are the following ones:

Linear actuator: is an actuator that creates motion in a straight line, in contrast to the circular motion of a conventional electric motor. Linear actuators are used in many places where linear motion is required. This actuator is the actual one, the one that moves the actual flap. In this new concept, it could be also used because it is easy to assemble, moves the flap, self-locks it and has the ability to send and receive information.

Servo motor: is a rotary actuator that allows for precise control of angular position, velocity and acceleration. It consists of a suitable motor coupled to a sensor for position feedback. It is a motor suitable for use in a closed-loop control system. As the linear actuator, it could be suitable for this project because it is easy to assemble, moves the flap, can self-lock the flap with a complement on it, has the ability to receive and send data. However, it is not able to rotate 360 degrees which can be a problem depending on the complement used to self-lock the flap.

Stepper motor: is a brush-less DC electric motor that divides a full rotation into a number of equal steps. The motor's position can then be commanded to move and hold at one of these steps without any position sensor for feedback (an open-loop controller), as long as the motor is carefully sized to the application in respect to torque and speed. As the other two actuator from above, the stepper motor is suitable to actuate the flap and fulfill all the requirements needed.

Figure 3.18: From left to right, linear actuator, servo motor and stepper motor. Source: robotshop.com, nextiafenix.com and nodna.de respectively

As seen above, all of them could be used with some complements to allow them to fulfill all the requirements. These complements could be an additional structure in the rod to allow the movement for the linear actuator, a brake for the servo motor and a worm gear for the stepper motor.

Since an additional structure is not sought, the idea of using the linear actuator has been discarded. Moreover, the brake for the servo motor is a disadvantage since it would consume energy while acting and what is wanted is fulfill all the requirements with nearly no energy consumed. Thus, the worm gear seems to be the best choice to keep the flap self-lock with consuming no energy. Since it is needed to be able to rotate 360 degrees because of the movement of the worm, the only option is using a stepper motor as the actuator of the flap (the servo motor, as said before, can not rotate these degrees).

Furthermore, using the worm gear as a complement, the torque needed in the actuator can be reduced due to gear ratio (For more information about gear ratio, see Appendix A - Study of the torque needed in the stepper motor worm gear). Thus, the weight can be also reduced.

To sum up, the final verdict is that stepper motor with a worm gear fits much better in the design. It is more suitable on this project because it fulfills all the requirements. It can accurately move the rod, giving the perfect deflection to the flap, self-lock the rod and, at the same time, the flap itself without consuming any type of energy and receive and send information to the main computer of the vessel.

Moreover, in order to give the stepper the ability of knowing all the time where the flap is even if it turns off, an encoder is going to be used.

Due to the power-needed calculations done (see Appendix A - Study of the torque needed in the stepper motor worm gear), the stepper has to have, at least, an output torque of 0.018 Nm.

The chosen stepper is a 0.26 Nm holding torque from RS (see data sheet in Appendix B: Stepper data sheet) and the worm gear reducer is the P20 with the gear ratio of 60:1 and self locking output from Ondrives with a P-X type single sided shaft (see data sheet in Appendix C: Worm gear reducer data sheet). In order to attach the stepper to the worm, a shaft rigid coupling from RS-components is used (also seen in the Appendix B: Stepper data sheet).

3.7.1 Shock Absorption System

During this long period of time sailing on its own, the Vane's flap has to be able to resist many different sorts of shocks. From a wave to a seagull impact, for instance. In order to be able to do that, a shock absorption system is needed.

This system has to be able to let the flap move due to the shock and, at the same time, keep save the actuator and the rest of the fragile parts of the flap design. There are many different types of shock absorption systems. However, the ones used in the remote control cars are the ones which have been looked at since the actuators of both of them (the cars and the flap) are quite similar.

Here, some shock absorption systems or, in other words, servo savers are exposed:

Figure 3.19: Servo saver examples. Source: fingertechrobotics.com

All of them are mainly composed by springs what make them be similar. Nevertheless, the one chosen is the one of the right because of its well performance and the possibility to regulate the force of the spring. If needed, the nut can rotate and compress the spring creating more strength of resistance.

In order to correctly adapt it to the requirements of the design, a new concept of servo saver has been created based on the one chosen before. Here, a sketch is shown:

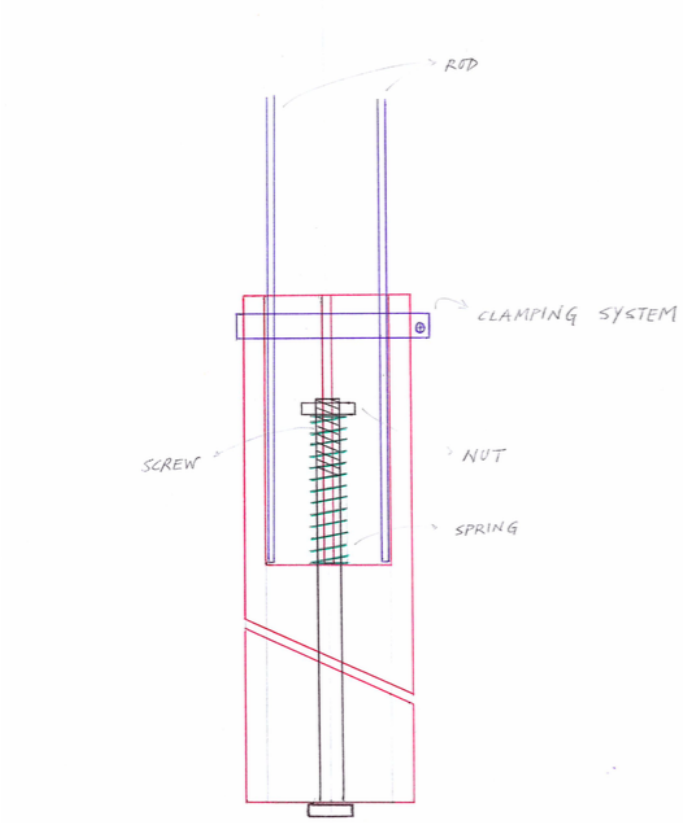

Figure 3.20: Sketch of the shock absorption system

Figure 3.21: Shock absorption system 3D printed prototype

This shock absorption system works in the following way: the spring from inside keeps both parts together and if an impact is received, bigger than the holding torque of the spring, it is compressed to let the upper part to move and prevent the actuator to feel it. This hypothetical impact could be created by a seagull or a wave, for instance. Since the flap is placed quite high in respect to the water line, a deep calculation about the possible impact of a seagull has been done (See Appendix D: Study of the torque created by an hypothetical seagull impact).

The result has been 1.45 Nm as the maximum torque created by this sort of impact. Since this value is higher than the maximum torque created by the wind (1.08 Nm), this last value has been taken as the limit where the spring has to start compressing itself in order to let the rod to move and prevent the actuator from damage.

Thus, the servo saver will not let movement between its own two parts while the torque is smaller than 1.08 Nm and that will allow the flap to stay on its ideal position resisting the force of the wind on its surface. But, if a higher than 1.08 Nm impact is created, the spring will be compressed and prevent the fragile parts of the system from big damage. The spring used is a 8 mm diameter one (For more information, see Appendix E: Study of shock absorption's spring force).

Moreover, the cut between the upper and lower part of the servo saver is 45 degrees. This gives the ability to always come back to the same initial position in case of rotation.

For more information about where it is placed and how, see 3.5.7 Electronics from above.

3.8 Manufacturing

3.8.1 Vacuum infusion

The Vacuum Infusion Process is one of many closed mold processes. It distinguishes itself by being the only process that utilizes only atmospheric pressure to push the resin into the mold cavity. The mold cavity can be a one-sided mold with bagging film being utilized for the "B" side, a two-sided mold, or even a soft "envelope" bag.

The process is highly controllable, due to it being governed by the principles of D'Arcy's Law (an equation that describes the flow of a fluid through a porous medium). This means that there are only three variables affecting the flow of the resin: (1) permeability of the laminate, (2) viscosity of the resin, and (3) pressure differential in the cavity in relation to atmospheric pressure. If all three of these variables are unchanged, then the infusion process will consistently flow the same way with every injection for a given part. This also equates to a very accurate bill of material for a given part since the resin and fiberglass usage will not change.

VIP brings all of the environmental advantages of a closed mold process, where styrene emissions are minimized due to the resin curing in a closed environment. It also provides an excellent glass-to-resin ratio with minimal to no voids in the finished laminate. This allows for one of the strongest ways of building a composite laminate.

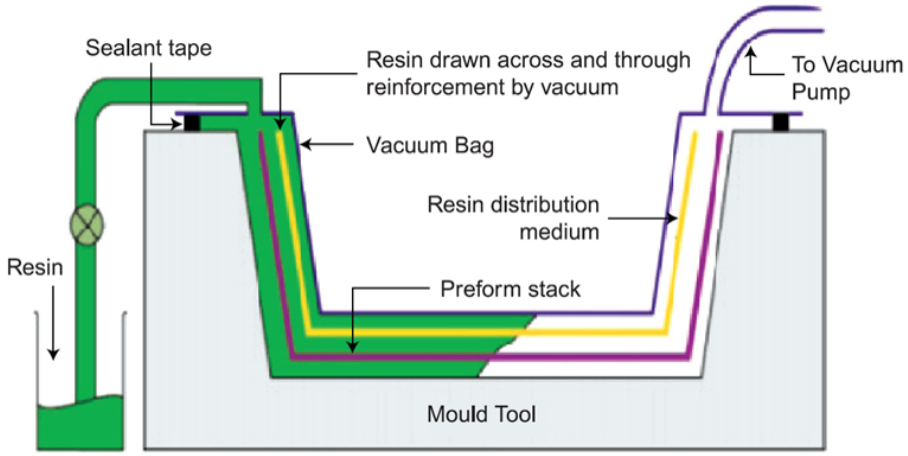

Figure 3.22: Vacuum infusion sketch. Source: netcomposites.com

The resin infusion process can be reduced to the following elements:

- A stack of dry material(s) to be laminated is placed in a leak-tight mold.
- A leak-tight flexible film (commonly known as a vacuum bag) is placed over the laminate and sealed to the mold beyond the perimeter of the laminate. Where multiples of the same part are to be made, the film may be molded to the shape of the part and be reusable.
- A minimum of two connections are made to the bag; one to permit air to be removed from the cavity between the bag and the mold and the other to allow liquid resin to enter.
- With the resin entry line temporarily closed, the cavity between the bag and the mold is evacuated by a vacuum pump. The level of vacuum necessary will vary depending on the permeability of the materials (i.e., with the ease by

which air and resin will flow through the materials) and by the complexity and desired quality of the final part. Except when the laminate could be damaged by excessive compression (e.g., a low density foam core), best results will be achieved by evacuating to the maximum level the vacuum pump is capable of – say to better than 95 per cent of the maximum possible vacuum.

- After this preliminary evacuation, the bag and mold should be temporarily closed off from the vacuum pump and the level of vacuum remaining in the part observed on a vacuum gauge. If the vacuum level remains constant, or at least reasonably constant, the mold and bag will be considered sufficiently leak-tight and the process can continue to the next stage. If, however, the vacuum level deteriorates at a faster level than can be accepted, air will be leaking into the evacuated cavity and the process should not continue.

  In this case, the air leaks must be found and eliminated before proceeding further. Acceptable leak back rates will vary depending on part size and desired laminate quality. For large parts such as boat hulls, a leak rate of less than 3 mbar/minute (approximately 1" Hg in 10 minutes) will be acceptable. For small, or critical parts an acceptable leak back rate might be 10 per cent of the above, say 3 mbar in 10 minutes, or 0.1" Hg in 10 minutes.
- Once a satisfactory level of leak-tightness has been achieved, the line to the vacuum pump can be reopened. The resin supply container can be filled with mixed resin and the line to the resin supply can be opened. With the resin supply line open, liquid resin will be forced into the part by the pressure difference between atmospheric pressure acting on the resin and the level of vacuum in the part, plus or minus the static head of the column of resin arising from the elevation of the resin supply relative to the part.

  If resin feed lines and vacuum off-takes have been correctly positioned on or around the dry laminate stack before the bag is placed, the liquid resin will seep or INFUSE through the whole laminate.
- Depending on the resin system used, the vacuum level during infusion may need to be regulated to a level lower than the vacuum pump is capable of. This particularly applies to resins containing volatile solvents which can boil under vacuum. Both polyester and vinyl ester resins should usually be infused at less than maximum vacuum.
- When thermosetting resins are used, a period of time must be allowed for the resin to cure after the laminate has been completely infused with resin. This time may vary from a few minutes to a few hours depending on the resin system and the size of the part.
- Once the resin has solidified, the bag and the part can be removed from the mold. The resulting part will be a homogeneous structure, with all components bound together within the resin matrix.

After all the vacuum infusion process, two totally homogeneous shells of carbon fiber have been obtained with which the flap assembly can be started.

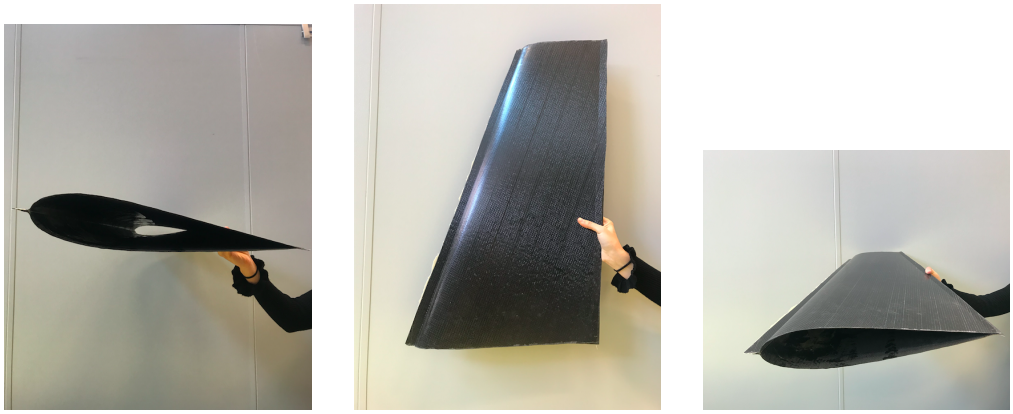

Figure 3.23: Views of the two shells of the flap

3.8.2 Assembly

One of the main requirements is the robustness. The assembly is one of the most critical part if the desired result is a robust flap. After thinking with different procedures of actuation the procedure followed to built the flap is the following one.

1. After doing the vacuum infusion the shells have been dried in a special oven for 8 hours at 85 degrees Celsius.
2. Two foam ribs are cut with to missions (1) to have more contact surface to stick the two shells together and (2) to attach the rod to the flap.
3. The outstanding part of the leading edge is sticked with epoxy glue after that is let it dry 24 hours.

Figure 3.24: Sticking the outstanding part of the leading edge with epoxy glue.

4. A piece of woven glass fiber is sticked in the inner of the trailing edge with the same resin used for the vacuum infusion in order to give strength to the leading edge when cutting the outstanding part. This process is dried for 24 hours.
5. The foam ribs are placed and glued with epoxy glue at the same time to the shells and to the rod.

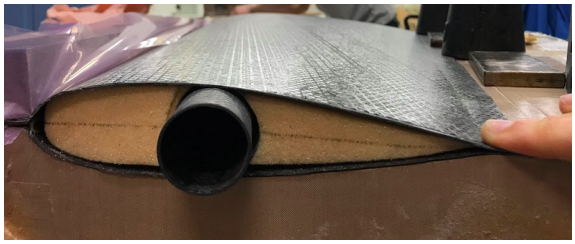

Figure 3.25: Top view of the flap with the top rib.

6. The outstanding part of the trailing edge is glued with epoxy glue. This process is dried for 24 hours.
7. A plate of carbon fiber is prepared with two layers of the fiber used for the shells of the flap. Two pieces are cut with the same dimensions of the NACA profile of the tops of the flap. The bigger piece (to cover the bottom of the flap) has a hole in the exact place where the rod is placed that fits perfectly with it. This two pieces are sticked with epoxy glue.
8. When everything is completely sticked and all the pieces have become all in one solid piece, the outstanding parts of the leading and trailing edges of the flap have been cut with a diamond blade. After that the margin that the blade has left is sanded by hand.

Figure 3.26: Cutting outstanding parts of the leading and trailing edges.

This assembly procedure so far has been done inside one of the molds in order to keep exactly the same shape.

9. All the joints of the flap have been covered with mastic made with the same resin used for the vacuum infusion mixed with aerosol and glass micro-spheres. The mix of all this products becomes a white mastic. This mastic has been mixed with black ink to get a dark silver color that fits on the original concept of the flap.

Figure 3.27: Side view of the flap with the silver mastic.

3.9 Final flap data

In the following table, it appears the most relevant specifications of the final flap.

Final flap data	
Profile	NACA0018
Span	75.0 cm
Root chord	42.0 cm
Root maximum thickness	7.6 cm
Tip chord	20.0 cm
Tip maximum thickness	3.6 cm
Leading edge angle	70º
Trailing edge angle	3.8º
Aspect Ratio	2.4
Taper Ratio	0.5
Material	carbon fiber
Weight of the fabric	440 g/m2
Number of layers	2
Lay up	0/+45/90/-45/-45/90/+45/0
Method	vacuum infusion
Number of ribs	2
Weight of the flap (without the rod)	450 g
Weight of the flap (with the rod)	850 g

Table 3.5: Final flap data

Chapter 4

Testing process

4.1 Comparative between old and new flap

In the following table, it is shown the most relevant differences between the old and the new flap.

Comparison	Old Flap	New Flap
Profile	NACA0018	NACA0018
Area [m2]	0.368	0.232
Aspect Ratio	5	2.42
Taper Ratio	1	0.48
Shell material	glass fiber	carbon fiber
Core material	foam	empty
Number of rods	2	1
Actuator	linear actuator	stepper
Weight	**1.50 kg**	**0.85 kg**

Table 4.1: Comparison between old and new flap

As it can be seen, the most important specification compared is that the new flap is much lighter than the old one. The weight has been reduced more than a 40 per cent from the old prototype. Also, having the new flap empty from inside and made with carbon fiber gives an extra value to its quality. The only thing that has been remained alike is the profile of the flap, NACA0018.

4.2 Evaluation

After the construction of the flap, Maribot VANE has been tested. The first test using the new flap took place at Stockholm Archipelago in the beginning of June. It was two days of testing with the authors of the thesis and other group members as well as supervisors who have been working in this project from the beginning.

Figure 4.1: Maribot VANE sailing with the new flap in Stockholm Archipelago

The Maribot VANE using the new flap has the same behavior as with the old flap with a naked eye. However, the The flap is 43 per cent lighter than the previous one, one of the main requirements of it. This has been done without losing robustness. It has rather been the contrary. Now all the electronics, joints, screws as well as the shock absorption system are covered inside the main wing. There is no any articulation in the inclemency. All this improvements make the flap a sight more robust.

Furthermore, due to the lightweight of the new flap, the moment of inertia of the entire rig around the Z axes is lower. The mass placed in the front can be located closer to the axes of rotation (half of the previous length).

This testing process has been just a first touchdown with the new flap. Owing to the early presentation of this bachelor's thesis after the construction of the flap, a complete aerodynamic study cannot be presented. Despite this, the team of the Maribot VANE continues testing this new flap in order to have exact results of the behavior of the entire rig to continue improving.

Chapter 5

Discussion, conclusion and future work

This chapter summarizes the thesis, discusses its findings and contributions, points out limitations of the current work, and also outlines directions for future research.

This thesis has developed a new an revolutionary flap for the Maribot VANE project, an autonomous sailing drone for oceanic research. This research project has been targeted by the Maritime Robotics Laboratory at The Royal Institute of Technology (KTH, Sweden) due to the actual accelerating need for oceanic sensing. All the work exposed along this thesis is the result of a hard and constant research work of the authors during more than three months.

Since the proposal of creating a new and optimized flap for the VANE came up, the authors have tried to create a new concept which fulfills all the requirements needed to improve on the old flap.

These ones were the following ones: to effectively generate a moment so that the rig is rotated to a desired angle of attack, to hold its position without any power consumption, to give a large restoring moment to stabilize the wing, to be a lightweight and robust structure, to be capable of keeping all the electronics needed to be moved protected from the water, to be connected/attached to the main wing, to have a shock absorption system and, finally, to be removable.

The thesis proofs that all these requirements have been fulfilled by the new flap concept. While testing the sailing drone at the Stockholm Archipelago, it was revealed that the flap is able to effectively generate the moment needed to reach equilibrium in a desired angle of attack for the main wing and that is also capable to give a large restoring moment to stabilize the wing if needed. Moreover, with the use of the stepper worm gear it can hold its position without any power consumption.

Furthermore, with the use of carbon fiber and having the structure empty from inside, a robust and lightweight structure has been created. The rod connects the flap to the main wing while transfers the movement created by the electronics from the watertight place inside the main wing to the flap. The hatch designed allows an easy way to remove and attach the flap to the main wing, to reach the electronics and to maintain the watertight protection inside the main wing.

Finally, the shock absorption mechanism designed makes the difference and fulfills the last requirement.

After testing the sailing drone in Sweden, the promising results of the new flap concept were verified. The Maribot VANE has the same behavior sailing as with the old flap while it gains lots of benefits. The area optimization which has reduced the original area by a 37 % has created a much more lightweight flap without losing robustness. In fact, on the contrary.

Moreover, due to the lightweight of the new flap, the moment of inertia of the whole rig around the Z axes is lower. Thus, the balance mass can be placed closer to the mast (axes of rotation). In fact, it can be located half of the previous distance.

Nevertheless, with this new design for the flap the problem found while sailing the very first time with the previous flap has not been solved but reduced. This problem was a very long swinging moment while sailing downwind. The new distribution of weight thanks to the new flap reduced its duration a bit. However, further study is needed in order to know where it comes from and why.

Finally, just stressing the fact that the team of the Maribot VANE at KTH continues working in this project in order to keep improving its design and behavior. Designing a collision system for the sailing drone or a new hull structure are examples of the future work.

Chapter 6

References

PAPERS

- U. Dhomé, C. Tretow, J. Kuttenkeuler, F. Wängelin, J. Fraize, M. Fürth, M. Razola, 2018. Development, and initial results of an autonomous sailing drone for oceanic research.
  Maritime Robotics Laboratory, KTH Royal Institute of Technology, Stockholm, Sweden.
  Davidson Laboratory, Stevens Institute of Technology, New Jersey, USA
  SSPA Sweden AB, Stockholm, Sweden
- Tretow, C, 2017, Design of a free-rotating wing sail for an autonomous sailboat, Master's thesis report, Centre for Naval Architecture, KTH Royal Institute of Technology, Stockholm.
- National Research Council, 2009. Science at Sea: Meeting Future Oceanographic Goals with a Robust Academic Research Fleet. Washington, DC: The National Academies Press
- Wängelin, F, 2017, Energy-efficient steering mechanism for an autonomous sailboat, Bachelor's thesis report, Center for Naval Architecture, KTH Royal Institute of Technology, Stockholm.

WEBSITES

- Airfoil Tools, 2018, [online] Avaliable at: www.airfoiltools.com [Acessed March 2018]
- Saildrone, 2018, [online] Available at: www.saildrone.com, [Accessed April 2018].
- Autonaut, 2018, [online] Available at: www.autonautusv.com [Accessed April 2018]
- Net Composites, 2018, [online] Avaliable at: www.netcomposites.com [Accessed June 2018]
- No Dna, 2018, [online] Avaliable at: www.nodna.de [Accessed March 2018]
- Nextiafenix, 2018, [online] Avaliable at: www.nextiafenix.com [Accessed March 2018]
- Robotshop, 2018, [online] Avaliable at: www.robotshop.com [Accessed March 2018]
- Fingertechorobotics, 2018, [online] Avaliable at: www.fingertechrobotics.com [Accessed April 2018]

Chapter 7

Appendix

7.1 Appendix A - Study of the torque needed in the stepper motor worm gear

In order to know the maximum torque needed, the lift for the worst situation has to be calculated. This worst conditions is considered as a super windy day of 60Kn.

It is known that the lift created in a NACA profile is equal to:

$$L = \frac{1}{2} \cdot \rho \cdot v^2 \cdot s \cdot Cl \tag{7.1}$$

where:

ρ = density of the wind = 1.225 Kg/m^3
v^2 = speed of the real wind = 60 Kn = 30.86 m/s
s = flap surface area = 0.2322 m^2
Cl = lift coefficient = for 4 degrees of angle of attack is 0.4

The value of the lift coefficient is taken from the graph of above (figure 3.7). The value of lift created for this condition is:

$$\textbf{L=54.18N} \tag{7.2}$$

With the aim of knowing the minimum torque needed in order the stepper motor to be able to move the flap in the desired angle of attack, the distance between the point where the lift is created in the profile and the position of the stepper is needed. The lift is created more or less at the 25 per cent of the chord of the profile. The stepper is placed nearly in the same horizontal position but in order to maximize a bit the calculation, 2 cm is considered as this distance. The torque, so, is equal to:

$$Torque = L \cdot d \tag{7.3}$$

Where:

L = lift created which is 54.18N as maximum in the worst situation.
d = distance between the point where the lift is created and the position of the stepper motor which is 2 cm.

$$\textbf{Minimum torque needed for the actuator = 1.08Nm} \tag{7.4}$$

Since a stepper worm gear is used with a gear ratio of 60:1, the torque needed in the actuator is much lower.

$$Ratio = \frac{v_{worm}}{v_{gear}} \cdot \frac{T_{gear}}{T_{worm}} \tag{7.5}$$

In the equation 7.10, it is seen how the torque and the speed are inversely proportional in a worm gear reducer system. With a ratio of 60:1, the worm has to do 60 turns to make the gear turn 360 degrees but the torque is the other way round. The torque in the output of the stepper has to be at least 0.018Nm to reach the 1.08Nm in the output of the gear. That allows to use a much smaller stepper as an actuator. Thus, reducing the weight too.

7.2 Appendix B: Stepper data sheet

RS PRO

Datasheet

ENGLISH

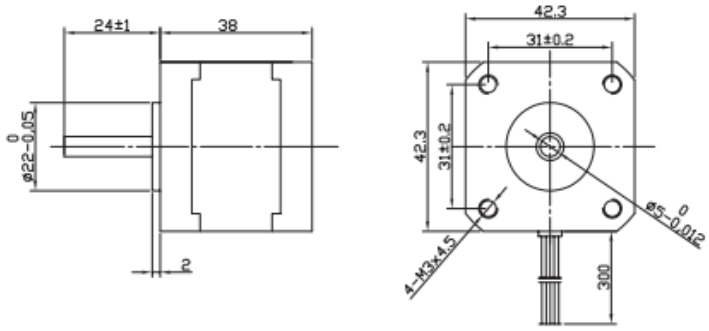

Characteristics

STEP ANGLE
1,8°

STEP ANGLE ACCURACY
± 5%

INSULATION CLASS
B

AMBIENT TEMPERATURE
-20°C +50°C

TEMP. RISE
80°C MAX (RATED CURRENT, 2 PHASE ON)

INSULATION RESISTANCE
100 M OHM MIN. 500 VDC

DIELECTRIC STRENGTH
500 VAC FOR ONE MINUTE

SHAFT RADIAL PLAY
0,02 MAX (450 G LOAD)

SHAFT AXIAL PLAY
0,08 MAX. (450 G LOAD)

MAX RADIAL FORCE
28 N (20 MM FROM FRONT FLANGE)

MAX AXIAL FORCE
10 N

Specification

Model		42SH38-1A	42SH38-2A	42SH38-3A	42SH38-4A
1 RATED VOLTAGE	V	4	6	12	2,8
2 CURRENT/PHASE	A	1,2	0,8	0,4	1,68
3 RESISTANCE/PHASE	Ω	3,3	7,5	30	1,65
4 INDUCTANCE/PHASE	MH	3,4	6,7	30	3,2
5 HOLDING TORQUE	NM	0,259	0,259	0,259	0,36
6 ROTOR INERTIA	G-CM²	54	54	54	54
7 WEIGHT	KG	0,28	0,28	0,28	0,28
8 NUMBER OF LEADS	N°	6	6	6	4

Speed vs. Torque Characteristics

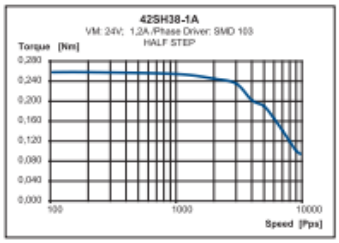

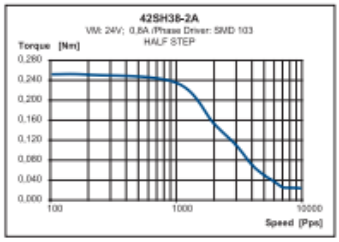

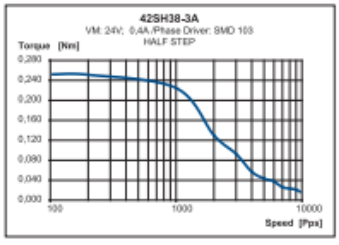

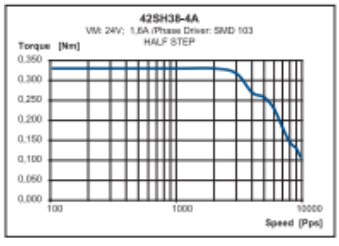

Connection

LEAD N°	COLOR	GAUGE	FUNCTION
1	BLACK	UL1430 AWG26	PHASE A
2	GREEN	UL1430 AWG26	PHASE A-
3	RED	UL1430 AWG26	PHASE B
4	BLUE	UL1430 AWG26	PHASE B-
	UNIPOLAR MOTOR		
5	YELLOW	UL1430 AWG26	COM PHASE A
6	WHITE	UL1430 AWG26	COM PHASE B

RS, Professionally Approved Products, gives you professional quality parts across all products categories. Our range has been testified by engineers as giving comparable quality to that of the leading brands without paying a premium price.

ONE- AND TWO-PIECE RIGID COUPLINGS

WITHOUT OR WITH KEYWAY · METRIC DIMENSION SERIES

MCLX/MSPX
MCLC/MSPC

MCLX

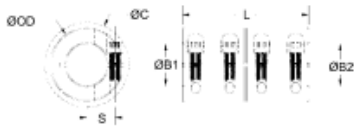

MCLC

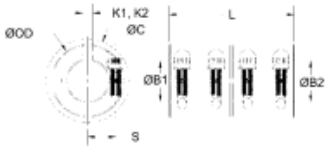

MSPX

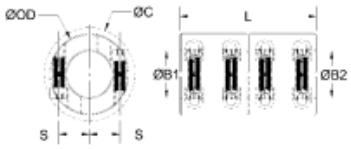

MSPC

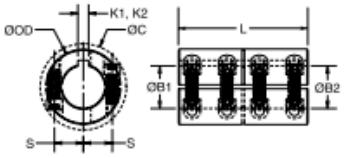

- Does not mar the shaft.
- Precision honed bore on straight bore couplings.
- 3-piece styles available.
- Nypatch® Anti-vibration hardware.
- Opposing hardware on 2-piece styles.
- Additional sizes available.
- Bore tolerance: +.050 mm +.012 mm
- Maximum speed: 4,000 rpm

PART NUMBER					SPECIFICATIONS							
ONE-PIECE			TWO-PIECE		BORES			SCREW	CLEARANCE	KEYWAY	FORGED
BLACK OXIDE STEEL	ALUMINUM	STAINLESS STEEL	BLACK OXIDE STEEL	STAINLESS STEEL	B1, B2 (mm)	OD (mm)	LENGTH L (mm)	LOC. S (mm)	DIAM. C (mm) MAX	K1, K2 (mm)	CLAMP SCREW
MCLX-3-3-F	MCLX-3-3-A	MCLX-3-3-SS	MSPX-3-3-F	MSPX-3-3-SS	3	15	22	4.6	15.0		M2
MCLX-4-4-F	MCLX-4-4-A	MCLX-4-4-SS	MSPX-4-4-F	MSPX-4-4-SS	4	15	22	4.6	15.0		M2
MCLX-5-5-F	MCLX-5-5-A	MCLX-5-5-SS	MSPX-5-5-F	MSPX-5-5-SS	5	15	22	4.6	15.0		M2
MCLX-6-6-F	MCLX-6-6-A	MCLX-6-6-SS	MSPX-6-6-F	MSPX-6-6-SS	6	18	30	5.9	21.5		M3
MCLX-8-8-F	MCLX-8-8-A	MCLX-8-8-SS	MSPX-8-8-F	MSPX-8-8-SS	8	24	35	9.0	27.1		M3
MCLX-10-10-F	MCLX-10-10-A	MCLX-10-10-SS	MSPX-10-10-F	MSPX-10-10-SS	10	29	45	10.6	33.0		M4
MCLX-12-12-F	MCLX-12-12-A	MCLX-12-12-SS	MSPX-12-12-F	MSPX-12-12-SS	12	29	45	10.6	33.0		M4
MCLX-14-14-F		MCLX-14-14-SS	MSPX-14-14-F	MSPX-14-14-SS	14	34	50	12.0	39.4		M5
MCLX-15-15-F		MCLX-15-15-SS	MSPX-15-15-F	MSPX-15-15-SS	15	34	50	12.0	39.4		M5
MCLX-16-16-F		MCLX-16-16-SS	MSPX-16-16-F	MSPX-16-16-SS	16	34	50	12.0	39.4		M5
MCLX-20-20-F		MCLX-20-20-SS	MSPX-20-20-F	MSPX-20-20-SS	20	42	65	15.4	48.9		M6
MCLX-25-25-F		MCLX-25-25-SS	MSPX-25-25-F	MSPX-25-25-SS	25	45	75	16.9	51.5		M6
MCLX-30-30-F		MCLX-30-30-SS	MSPX-30-30-F	MSPX-30-30-SS	30	53	83	20.9	58.7		M6
MCLX-35-35-F		MCLX-35-35-SS	MSPX-35-35-F	MSPX-35-35-SS	35	67	95	26.7	74.7		M8
MCLX-40-40-F		MCLX-40-40-SS	MSPX-40-40-F	MSPX-40-40-SS	40	77	108	31.8	84.0		M8
MCLX-50-50-F		MCLX-50-50-SS	MSPX-50-50-F	MSPX-50-50-SS	50	85	124	34.1	94.2		M10
MCLC-6-6-F		MCLC-6-6-SS	MSPC-6-6-F	MSPC-6-6-SS	6	18	30	5.9	21.5	2	M3
MCLC-8-8-F		MCLC-8-8-SS	MSPC-8-8-F	MSPC-8-8-SS	8	24	35	9.0	27.1	2	M3
MCLC-10-10-F		MCLC-10-10-SS	MSPC-10-10-F	MSPC-10-10-SS	10	29	45	10.6	33.0	3	M4
MCLC-12-12-F		MCLC-12-12-SS	MSPC-12-12-F	MSPC-12-12-SS	12	29	45	10.6	33.0	4	M4
MCLC-14-14-F		MCLC-14-14-SS	MSPC-14-14-F	MSPC-14-14-SS	14	34	50	12.0	39.4	5	M5
MCLC-15-15-F		MCLC-15-15-SS	MSPC-15-15-F	MSPC-15-15-SS	15	34	50	12.0	39.4	5	M5
MCLC-16-16-F		MCLC-16-16-SS	MSPC-16-16-F	MSPC-16-16-SS	16	34	50	12.0	39.4	5	M5
MCLC-20-20-F		MCLC-20-20-SS	MSPC-20-20-F	MSPC-20-20-SS	20	42	65	15.4	48.9	6	M6
MCLC-25-25-F		MCLC-25-25-SS	MSPC-25-25-F	MSPC-25-25-SS	25	45	75	16.9	51.5	8	M6
MCLC-30-30-F		MCLC-30-30-SS	MSPC-30-30-F	MSPC-30-30-SS	30	53	83	20.9	58.7	8	M6
MCLC-35-35-F		MCLC-35-35-SS	MSPC-35-35-F	MSPC-35-35-SS	35	67	95	26.7	74.7	10	M8
MCLC-40-40-F		MCLC-40-40-SS	MSPC-40-40-F	MSPC-40-40-SS	40	77	108	31.8	84.0	12	M8
MCLC-50-50-F		MCLC-50-50-SS	MSPC-50-50-F	MSPC-50-50-SS	50	85	124	34.1	94.2	14	M10

FOR ENGINEERING AND WARRANTY INFORMATION SEE WWW.RULAND.COM

www.ruland.com · Phone (508) 485-1000 · Fax (508) 485-9000

7.3 Appendix C: Worm gear reducer data sheet

P20 | **CAD Drawings Available On Request**

PRECISION GEARBOXES

Worm Gear Reducers

Shaft Input : 1.25Nm to 5Nm : ***5:1 - 120:1***

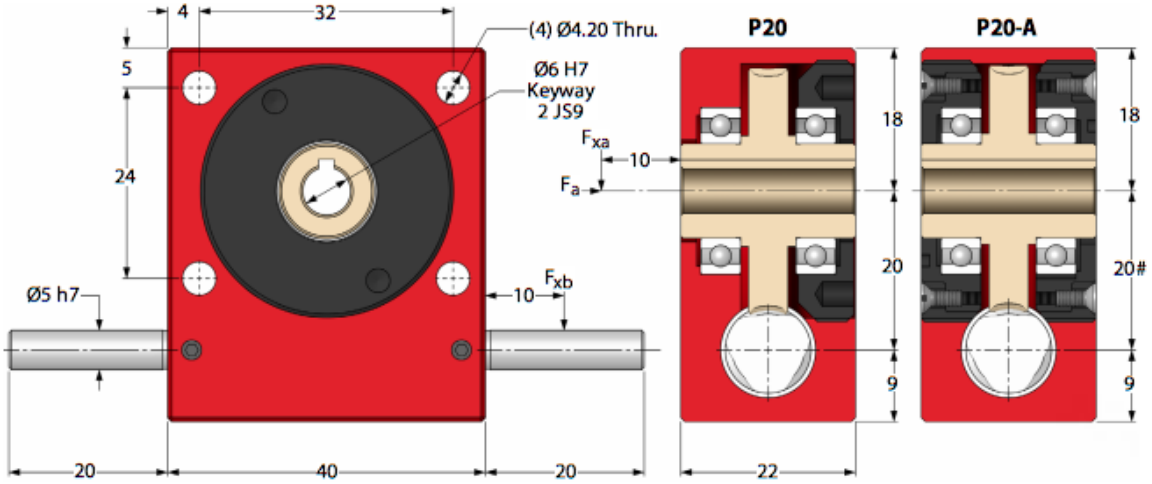

P20A version (low backlash) output is on eccentric so centres will vary.

Standard ≤30'	Part Number Low Backlash ≤8'	Red. Backlash ≤4'	Ratio	Efficiency at 1000 Rpm	Reflected Inertia at Input (kg.m²)	Self Locking Output
P20-10	P20-10A	P20-10AR	10:1	86%	2.03×10^{-7}	✗
P20-12	P20-12A	P20-12AR	12:1	85%	1.93×10^{-7}	✗
P20-15	P20-15A	P20-15AR	15:1	84%	1.85×10^{-7}	✗
P20-20	P20-20A	P20-20AR	20:1	78%	1.78×10^{-7}	✗
P20-30	P20-30A	P20-30AR	30:1	71%	1.74×10^{-7}	✗
P20-60	P20-60A	P20-60AR	60:1	60%	1.71×10^{-7}	✓
P20-120	P20-120A	P20-120AR	120:1	32%	1.50×10^{-7}	✓

Other ratios between 5:1 and 120:1 are available to special order.
Input shaft modifications also available: Single shafts • shorter lengths • smaller diameters • milled Keyways & flats • circlip grooves • pin holes.

Weight: 0.18kg.
Maximum Input Overhung Load at 1,000 rpm (F_{xb}): 6kg.
Maximum Output Overhung Load at 1,000 rpm (F_{xa}): 12kg.
Maximum Output Thrust Load at 1,000 rpm (F_a): 5kg.

Precision reduction worm and wheel gearbox with aluminium casing. Grease filled for life.
Right hand lead worm and wormwheel as standard. Left hand can be supplied on request.
Custom units can be supplied to suit a wide range of applications and requirements.

Self locking output is subject to ratio and only applies in static condition.
Amount of locking effect may vary due to manufacturing processes.

Testing in your applications is necessary. You will need to assess duty cycles and confirm gearbox suitability with your own calculations. All figures listed are for guidance only.

Rpm Input	Output Torque Nm Reduction Ratio 10:1	12:1	15:1	20:1	30:1	60:1	120:1
3000	1.40	1.50	1.60	1.70	1.90	2.10	1.25
2000	1.70	1.70	1.80	1.80	2.10	2.40	1.42
1000	2.10	2.30	2.30	2.50	2.70	2.90	1.70
500	2.70	2.70	2.80	2.90	3.20	3.50	1.94
200	3.40	3.50	3.50	3.70	3.90	4.10	2.27
100	3.90	3.90	4.10	4.20	4.30	4.50	2.55
50	4.40	4.50	4.50	4.60	4.70	4.80	2.72
10	4.80	4.80	4.90	4.90	5.00	5.00	2.72

P-X
P-DX

CAD Drawings Available On Request

PRECISION GEARBOXES

Gearbox Output Shafts

Single & Double Sided For P & PF Type Worm Gear Reducers

P-X Type Single Sided

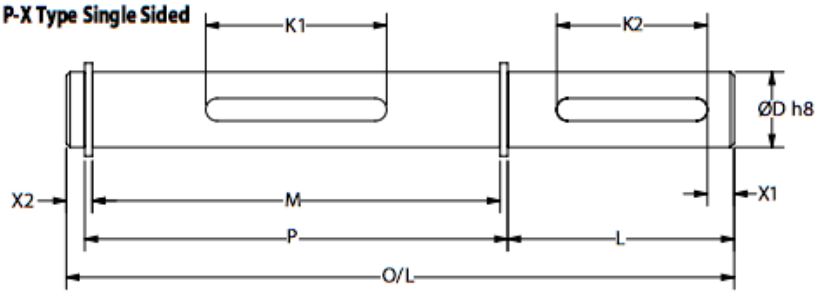

P-DX Type Double Sided

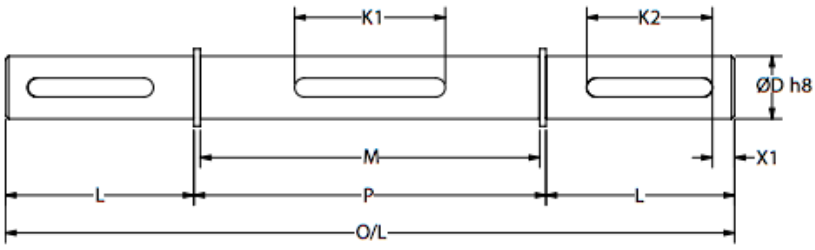

Part Number	ØD	O/L	M	P	L	To Suit Key K1	X1	To Suit Key K2	X2
SINGLE									
P15-X	6	50.8	22	23.6	25	KK2-20	1.50	KK2-20	3.0
P20-X	6	50.8	22	23.6	25	KK2-20	1.50	KK2-20	3.0
P30-X	8	63.9	28	29.8	32	KK2-22	3.00	KK2-22	3.0
P40-X	10	76.6	32	34.2	40	KK3-20	3.50	KK3-20	3.5
P45-X	12	88.1	38	40.2	45	KK4-25	4.00	KK4-25	4.0
P55-X	15	101.1	46	48.2	50	KK5-30	4.00	KK5-30	4.0
P60-X	20	119.8	54	56.6	60	KK6-32	4.00	KK6-32	4.5
P70-X	25	135.8	60	62.6	70	KK8-40	4.50	KK8-40	4.5
DOUBLE									
P15-DX	6	73.6	22	23.6	25	KK2-20	1.50	KK2-20	-
P20-DX	6	73.6	22	23.6	25	KK2-20	1.50	KK2-20	-
P30-DX	8	93.8	28	29.8	32	KK2-22	5.45	KK2-22	-
P40-DX	10	114.2	32	34.2	40	KK3-20	9.90	KK3-20	-
P45-DX	12	130.2	38	40.2	45	KK4-25	4.00	KK4-25	-
P55-DX	15	148.2	46	48.2	50	KK5-30	9.90	KK5-30	-
P60-DX	20	176.6	54	56.6	60	KK6-32	13.75	KK6-32	-
P70-DX	25	202.5	60	62.6	70	KK8-40	14.90	KK8-40	-

Stainless Steel shaft. Steel keys and circlips included.
Special shafts to your own design are available, P.O.A. Please fax a drawing for a quote.

7.4 Appendix D: Study of the torque created by an hypothetical seagull impact

In order to know how much torque would create an hypothetical case of a seagull impact in the flap and how the flap has to be designed to support it, a calculation for this possible situation is needed. Since the flap has to be able to resist this impact, the worst condition has been taken as scenario, a big seagull with high speed and impacting in the trailing edge of the flap.

$$Force = mass \cdot acceleration \tag{7.6}$$

where:

mass = 2 Kg (weight of a big/fat seagull)
speed = 45 Km/h (around maximum speed a seagull can fly)
time = 5 s (around minimum time it needs to reach that speed)

Thus, an impact of a seagull would create a force of 5N.
To know the torque created in the flap,

$$Torque = force \cdot distance \tag{7.7}$$

where:

force = 5N
distance = 0.29 meters

According to this equation, the torque created by the impact of the bird would be around **1.45Nm** in the worst case.

7.5 Appendix E: Study of the force needed in the shock absorption's spring

The shock absorption has to actuate when the torque created by the maximum wind condition is reached. According to the calculations done before (See Appendix A), this value is 1.08Nm. Thus, when the torque is bigger than this number, the spring of the servo saver has to be able to let the upper piece move and, at the same time, to protect the actuator. The situations when the torque can be bigger than 1.08Nm are the ones exposed before, seagull (Appendix D) or a wave impact.

In this calculation the torque limit is the maximum torque created by the wind (1.08Nm) not the maximum created by the impact of the seagull since the first one is smaller.

$$Torque_{wind} = Torque_{spring} \tag{7.8}$$

$$1.08Nm = \eta \cdot F_{normal} \cdot distance \tag{7.9}$$

Because the normal force is created by the spring, this force is composed by the K and its compression x,

$$1.08Nm = \eta \cdot K \cdot x \cdot distance \tag{7.10}$$

Because of its geometry,

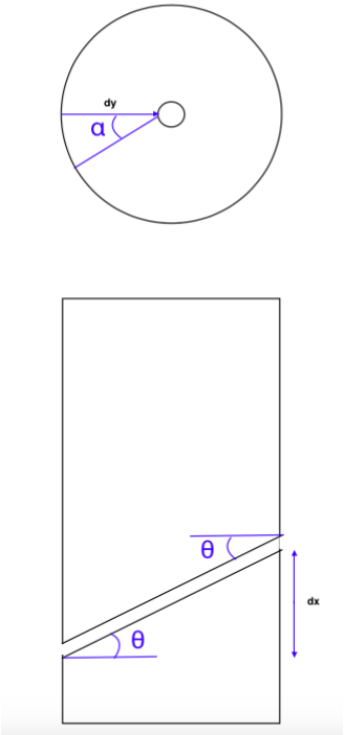

Figure 7.1: Sketch of the geometry of the shock absorption

$$F = K \cdot x \tag{7.11}$$
$$dx = \tan(\alpha) \cdot dy \tag{7.12}$$
$$dy = (r - r \cdot \cos(\theta)) \tag{7.13}$$
$$F(\theta) = K \cdot \tan(\alpha) \cdot (r - r \cdot \cos(\theta)) \tag{7.14}$$

Thus,

$$1.08Nm = \eta \cdot K \cdot \tan(\alpha) \cdot (r - r \cdot \cos(\theta)) \cdot distance \tag{7.15}$$

where:

η = friction coefficient of Nylon (friction surface material) = 0.06
α = depends on the movement of the shock absorption
r = 0.041 m
θ = 22.5º
distance = width/radius of the spring = 0.004 m

So,

$$K = \frac{1.500.000}{\tan(\alpha)} \tag{7.16}$$

7.6 Appendix F: Study of the bending stress and deflection of the rods

In order to know which rods have to be used, a study of the bending stress and deflection has to be done. Carbon fiber has been taken as the material for these rods due to its low weight and high resistance properties. The study is based on comparing different rods offered by a Swedish company, Carbix. The formulas used to calculate the bending stress and the deflection are the following ones:

$$M_{inertia} = \frac{(\pi \cdot (\emptyset^4_{exterior} - \emptyset^4_{interior})}{64} \tag{7.17}$$

$$Deflection = \frac{L^3 \cdot F}{3 \cdot E \cdot M_{inertia}} \tag{7.18}$$

$$Bending = \frac{F \cdot L \cdot 0.5 \cdot t}{M_{inertia}} \tag{7.19}$$

where:

L = length of the tube beam, 1 meter in all cases
F = force applied, for all the cases 54.18 N as the worst case
E = Young's modulus, for carbon fiber = 228 GPa
t = thickness

Thus, the deflection and bending stress values for each rod are the following ones:

- Rod 1 ($\emptyset_{exterior} = 21.5mm, \emptyset_{interior} = 19.5mm$)
  Deflection = 29.00 mm
  Bending stress = 173.35 MPa
- Rod 2 ($\emptyset_{exterior} = 24mm, \emptyset_{interior} = 22mm$)
  Deflection = 20.32 mm
  Bending stress = 137.21 MPa
- Rod 3 ($\emptyset_{exterior} = 26.4mm, \emptyset_{interior} = 24.5mm$)
  Deflection = 15.20 mm
  Bending stress = 111.98 MPa
- Rod 4 ($\emptyset_{exterior} = 29.5mm, \emptyset_{interior} = 26.9mm$)
  Deflection = 8.51 mm
  Bending stress = 70.05 MPa
- Rod 5 ($\emptyset_{exterior} = 32.5mm, \emptyset_{interior} = 29.9mm$)
  Deflection = 6.26 mm
  Bending stress = 56.82 MPa

The final choice is using the two less deflected rods, Rod 4 and 5, since the bending stresses are quite low comparing to the tensile strength of the carbon fiber (around 2000 MPa depending on the layers and resin used in the composite). The widest one, Rod 5, will be used as a rail to the other one, Rod 4, which will hold the flap.

7.7 Appendix G: Flap CAD